NOAA TM ERL ARL-28

A UNITED STATES DEPARTMENT OF COMMERCE PUBLICATION

NOAA Technical Memorandum ERL ARL-28

U.S. DEPARTMENT OF COMMERCE
NATIONAL OCEANIC AND ATMOSPHERIC ADMINISTRATION
Environmental Research Laboratories

Atmospheric Transport and Diffusion in the Planetary Boundary Layer January - July 1970

Air Resources Laboratories
SILVER SPRING, MARYLAND
January 1971

ENVIRONMENTAL RESEARCH LABORATORIES

AIR RESOURCES LABORATORIES

IMPORTANT NOTICE

Technical Memoranda are used to insure prompt dissemination of special studies which, though of interest to the scientific community, may not be ready for formal publication. Since these papers may later be published in a modified form to include more recent information or research results, abstracting, citing, or reproducing this paper in the open literature is not encouraged. Contact the author for additional information on the subject matter discussed in this Memorandum.

NATIONAL OCEANIC AND ATMOSPHERIC ADMINISTRATION

U.S. DEPARTMENT OF COMMERCE
National Oceanic and Atmospheric Administration
Environmental Research Laboratories

NOAA Technical Memorandum ERL ARL-28

ATMOSPHERIC TRANSPORT AND DIFFUSION IN THE PLANETARY BOUNDARY LAYER JANUARY - JULY 1970

I. Van der Hoven, Editor

Contributors

J. K. Angell
A. B. Bernstein
D. J. Bjorem
C. R. Dickson
D. H. Pack
D. H. Slade
G. E. Start
L. L. Wendell

Semiannual Research Program Review

January - July 1970

U. S. Atomic Energy Commission

Air Resources Laboratories
Silver Spring, Maryland
January 1971

PREFACE

In accordance with the letter of agreement of July 24, 1969, with the U. S. Atomic Energy Commission, Division of Reactor Development and Technology, the Air Resources Laboratories have continued their study of atmospheric transport and diffusion in the planetary boundary layer, micrometeorology, diffusion climatology, and the application of this work to the disposal of radioactive waste gases into the atmosphere. The research is technically administered and supervised through the Air Resources Environmental Laboratory of the Air Resources Laboratories. The work is performed at the Air Resources Headquarters in Silver Spring, Maryland, and at the Air Resources Idaho Falls Laboratory, National Reactor Testing Station, Idaho. Any inquiry on the research being performed should be directed to the editor, Isaac Van der Hoven, Chief, Air Resources Environmental Laboratory, Air Resources Laboratories, National Oceanic and Atmospheric Administration, 8060 - 13th Street, Silver Spring, Maryland 20910.

TABLE OF CONTENTS

		Page
1.	RESEARCH AT AIR RESOURCES LABORATORIES HEADQUARTERS, SILVER SPRING, MD.	1
	1.1 Mesoscale Lagrangian Studies (Tetroon Research)	1
	1.1.1 Lagrangian-Eulerian Relationships	1
	1.1.2 Urban Wind Structure Studies	3
	1.1.3 The Representativeness of Reynolds Stresses From Tetroon Flights	8
	1.1.4 Urban Wind and Air Pollution Studies	10
	1.2 Mixing Length Hypotheses	11
	1.3 Planetary Boundary Layer Dynamics	11
2.	RESEARCH AT THE NATIONAL REACTOR TESTING STATION, IDAHO	12
	2.1 Mesoscale Transport Studies	12
	2.1.1 Comparisons of Trajectories Derived From Wind Fields and Single Station Wind Data	12
	2.1.2 Trajectory Statistics for Selected Receptors	16
	2.1.3 Error Checking and Correction	23
	2.1.4 Comparison of Tetroon and Wind Field Trajectories	25
	2.1.5 Animation of Trajectory Plots	30
	2.2 Mesoscale Forecast	32
	2.3 The Surface Winds at CFA	38
	2.4 Aircraft Wake Turbulence Interagency Study	41
3.	REFERENCES	43
APPENDIX A		45
A1.	PUBLICATIONS AND REPORTS	46
A2.	LABORATORY PERSONNEL	47

ATMOSPHERIC TRANSPORT AND DIFFUSION IN THE PLANETARY BOUNDARY LAYER

AIR RESOURCES LABORATORIES SEMIANNUAL RESEARCH PROGRAM REVIEW FOR THE ENVIRONMENTAL SAFETY BRANCH DIVISION OF REACTOR DEVELOPMENT AND TECHNOLOGY U. S. ATOMIC ENERGY COMMISSION

JANUARY - JULY 1970

1. RESEARCH AT AIR RESOURCES LABORATORIES HEADQUARTERS, SILVER SPRING, MD.

1.1 Mesoscale Lagrangian Studies (Tetroon Research)

This is a joint research effort of several Air Resources Laboratories with the sponsorship of both the Atomic Energy Commission (AEC) and the National Air Pollution Control Administration (NAPCA).

1.1.1 Lagrangian-Eulerian Relationships

The Lagrangian-Eulerian scale ratios derived from constant volume balloon (tetroon) flights past the 1500-ft BREN tower at the Nevada Test Site and from fixed anemometry on the tower have been analyzed for a number of turbulence parameters. Figure 1 compares fixed point or Eulerian (dashed lines) and tetroon-derived or Lagrangian (solid lines) vertical velocity spectra, where the spectra in each diagram represent the composite of 12 individual spectra grouped according to designated ranges of lapse rate, wind speed, root mean square (rms) vertical velocity, and vertical turbulence intensity. In general, Lagrangian spectral peaks (solid arrows) occur at lower frequencies than the Eulerian spectral peaks (dashed arrows). For several of the more stable groups at the top of the figure, the lower frequency Lagrangian spectral peak was chosen because of suspected radar positioning errors causing the high frequency peak. The basic spectral data involved 30-sec average values of the vertical velocity component.

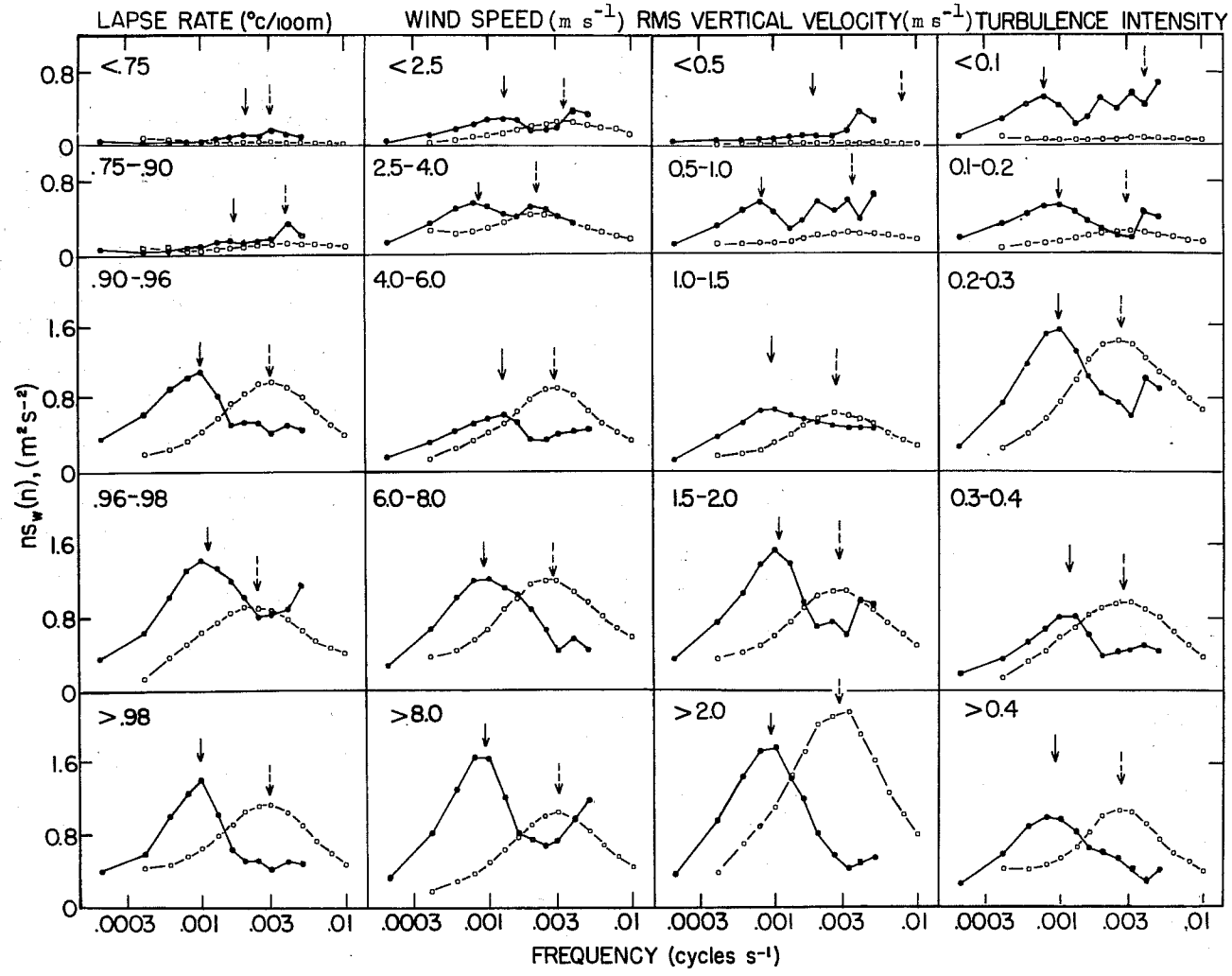

Figure 1. Eulerian (dashed line) and Lagrangian (solid line) vertical velocity spectra at the BREN tower composited according to values of lapse rate, wind speed, rms vertical velocity, and vertical turbulence intensity. The group limits are shown at the upper left; the vertical arrows indicate the respective spectral peaks.

Figure 2 shows the derived variation of the Lagrangian-Eulerian scale ratio with variation in the above parameters. The ratio increases with an increase in lapse rate (more unstable) and wind speed, and decreases with an increase in rms vertical velocity and vertical turbulence intensity. In the latter case the ratio is indicated as decreasing from a value of 4.5 at a turbulence intensity of 0.05 to a value of 2.5 at turbulence intensities exceeding 0.3. The maintenance of the ratio at relatively high turbulence intensities should be viewed with caution, because during such times the mean tetroon height was above the tower where fixed point measurements were made.

1.1.2 Urban Wind Structure Studies

The analysis of the data obtained from the low-level tetroon flights in March 1969 across downtown Columbus, Ohio, has been largely completed. Of considerable interest is the evidence that at heights of 100-200 m the city induces an anticyclonic turning of the trajectories in the mean. Figure 3

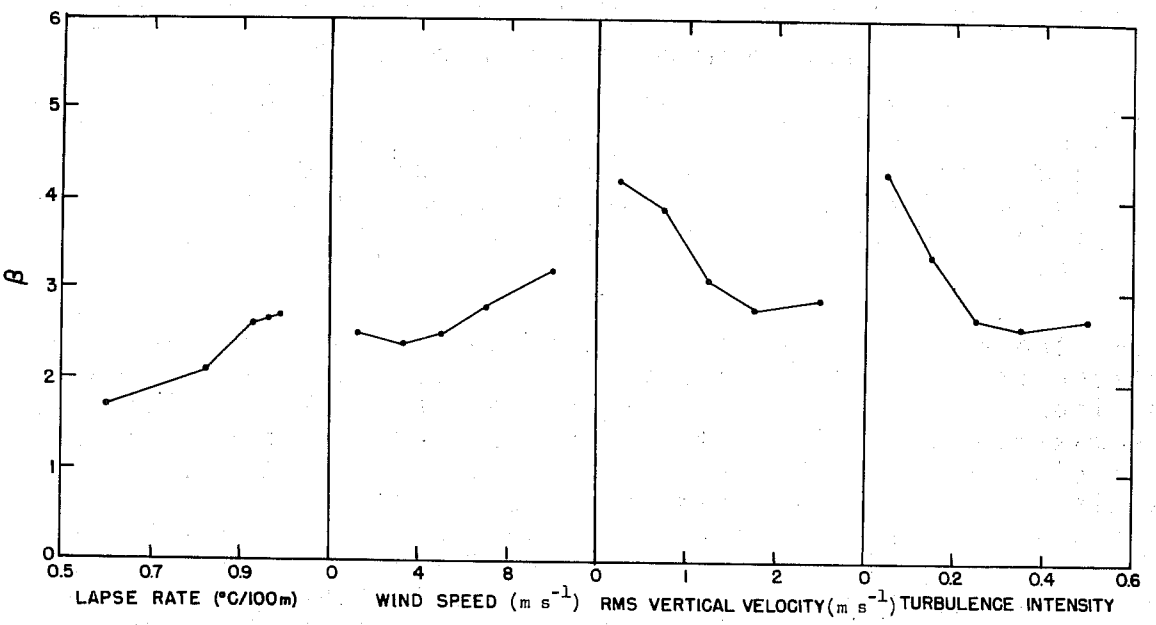

Figure 2. Variation of the Lagrangian-Eulerian time scale ratio, β, with lapse rate, wind speed, rms vertical velocity, and vertical turbulence intensity at the BREN tower.

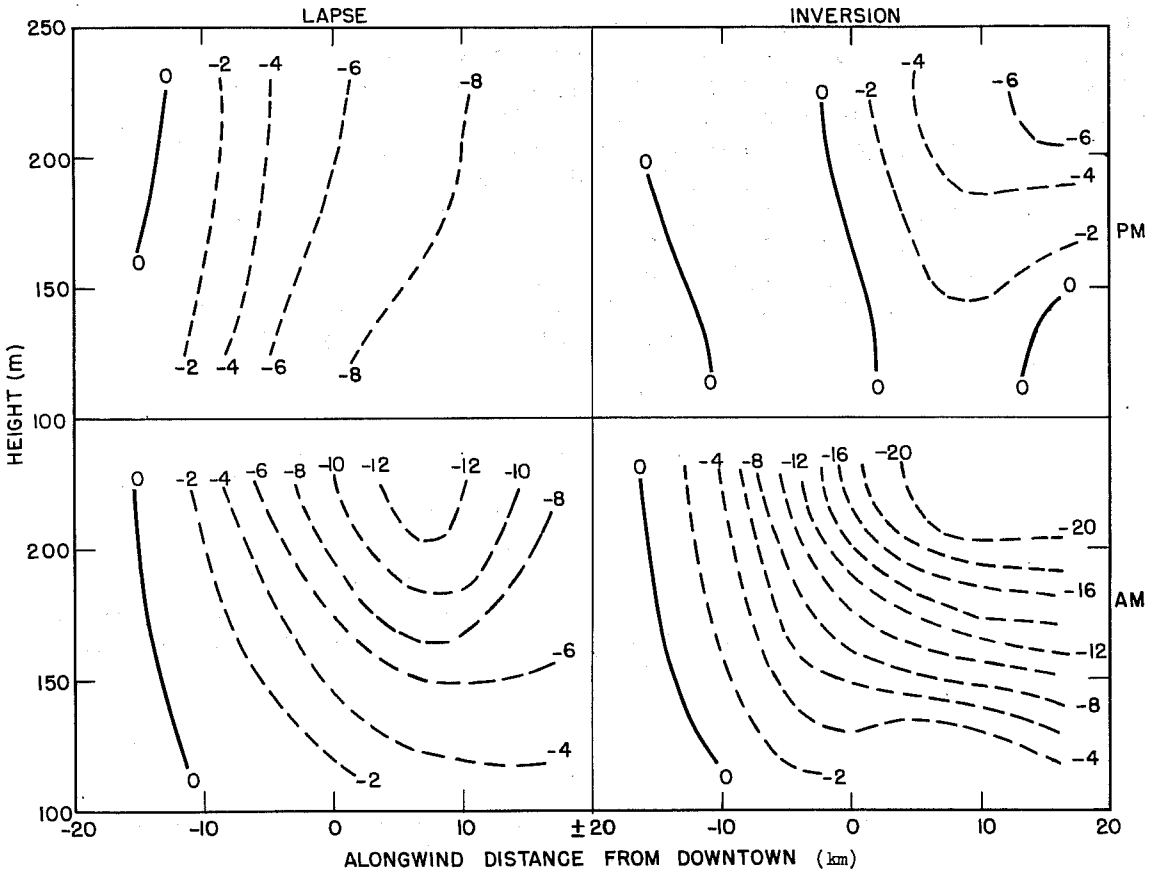

Figure 3. Total change in wind direction in degrees from the value at 16 km upwind (negative abscissa values) of downtown determined from tetroon flights across Columbus, Ohio, in lapse and inversion conditions before and after midnight. Negative numbers and dashed lines indicate an anticyclonic turning.

shows the average wind direction change in degrees along the tetroon trajectories as the tetroons pass over the city during lapse and inversion conditions before and after midnight. The maximum anticyclonic trajectory curvature tends to occur near city center, offering strong evidence that the turning is city induced. After midnight the anticyclonic turning increases with height between 100 and 200 m. Presumably reflecting the formation of a mesoscale high above the city due to the warmer temperatures within the city (the urban heat island effect). The anticyclonic turning before midnight is believed mainly due to an increase in the frictional force resulting from increased vertical mixing over the city. Figure 4 shows the frictional force (F) over the city under lapse and inversion conditions at heights of 100 and 200 m obtained from the residual of the Coriolis force (C) and

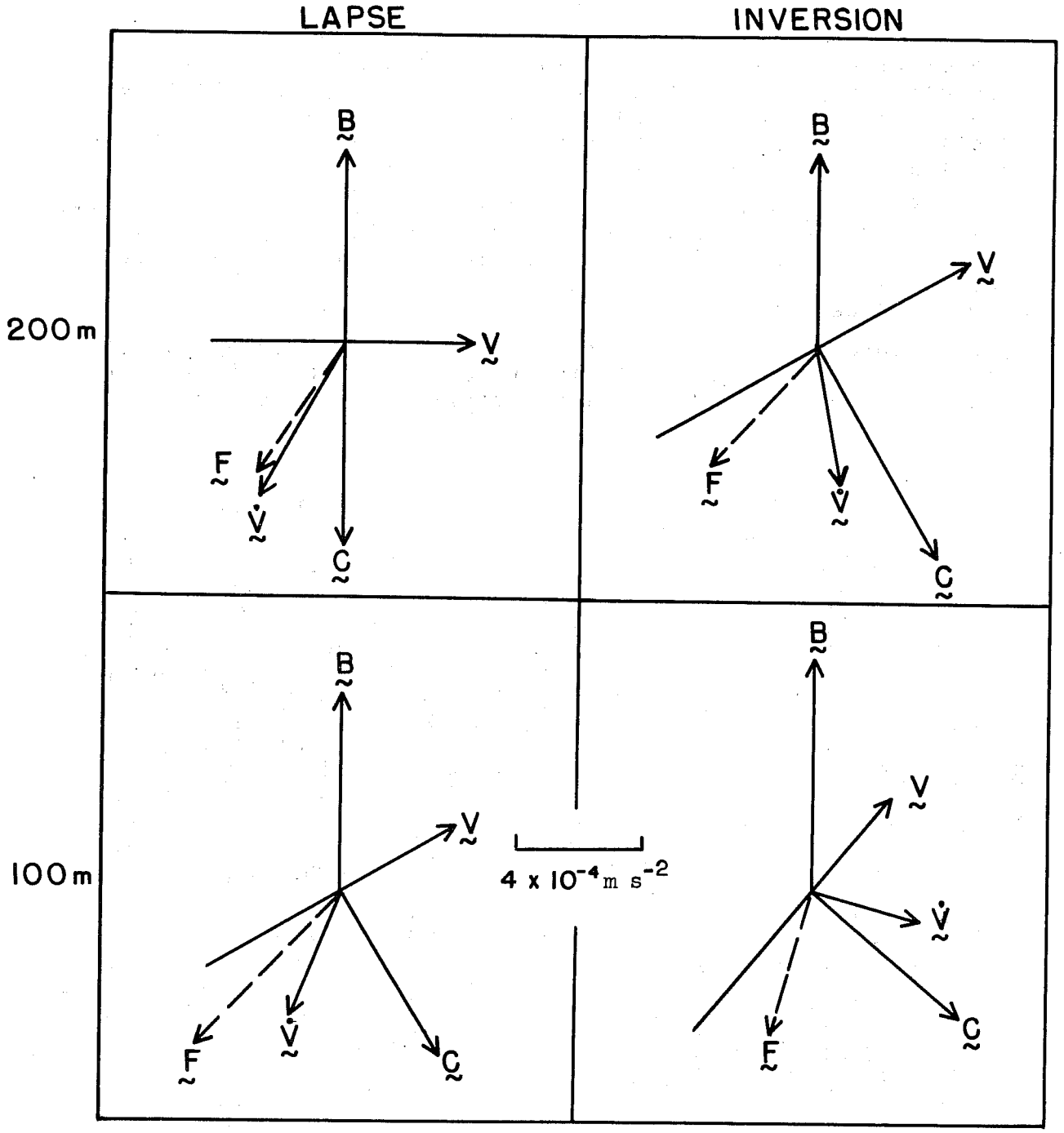

Figure 4. Balance of specific pressure gradient force B, specific Coriolis force C, tetroon-derived individual acceleration V̇, and derived specific frictional force F in relation to tetroon velocity V, in lapse and inversion conditions near 100 and 200 m above Columbus, Ohio. All force parameters are evaluated in the horizontal plane; the specific force scale is given at the center bottom.

acceleration ($\dot{V}$) derived from the tetroons and the pressure gradient force (B) derived from surface pressures. It is apparent that in all cases an increase in the magnitude of the frictional force would result in increased anticyclonic turning if all other forces were held constant.

Figure 5 shows the wind deceleration induced by the city. As expected, the deceleration is appreciable (as much as 40 percent of the upwind speed) under lapse conditions but negligible under inversion conditions. In all cases the region of maximum deceleration tilts downwind with height.

Figure 6 shows the vertical velocity induced by the city under conditions of light to moderate wind speed. An average upward motion of about 4 cm sec^{-1} occurs above the city in

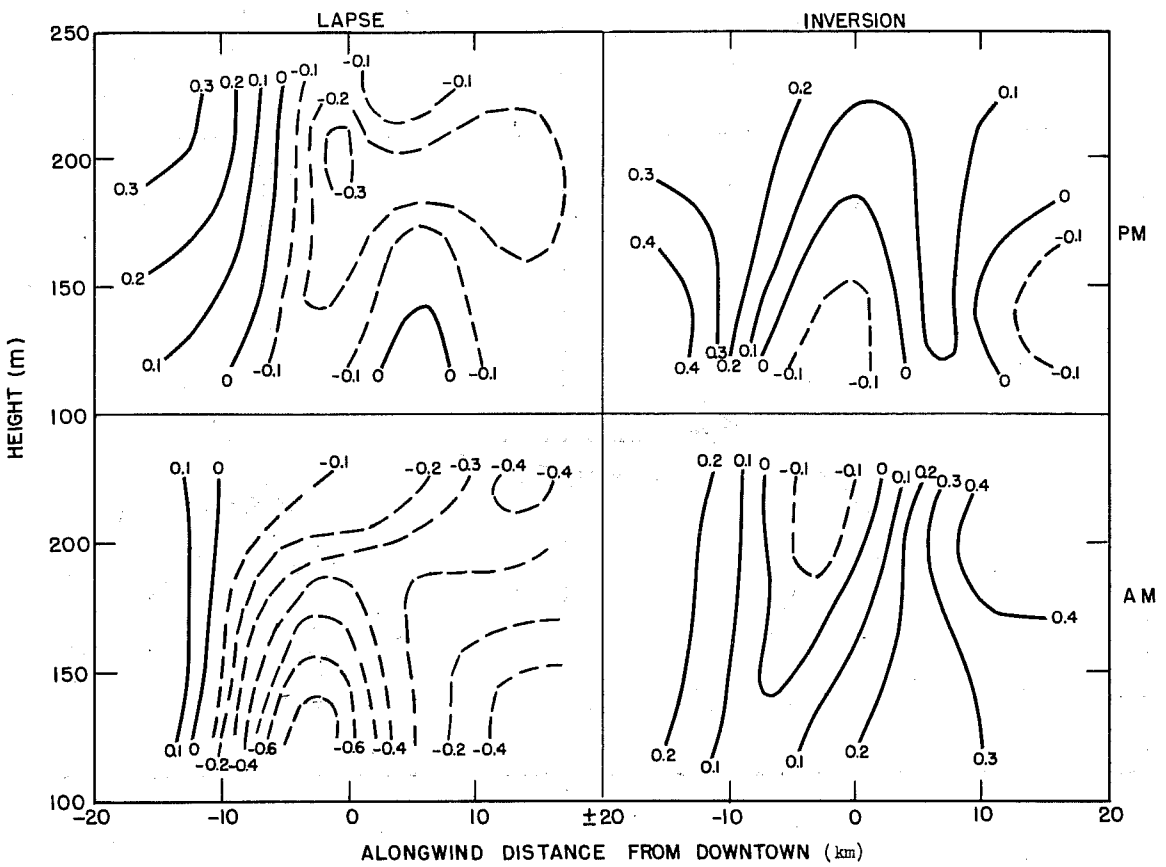

Figure 5. Spatial wind accleration (m sec^{-1} per 4 km) determined from tetroon flights across Columbus, Ohio, under lapse and inversion conditions before and after midnight. Negative numbers and dashed lines indicate deceleration.

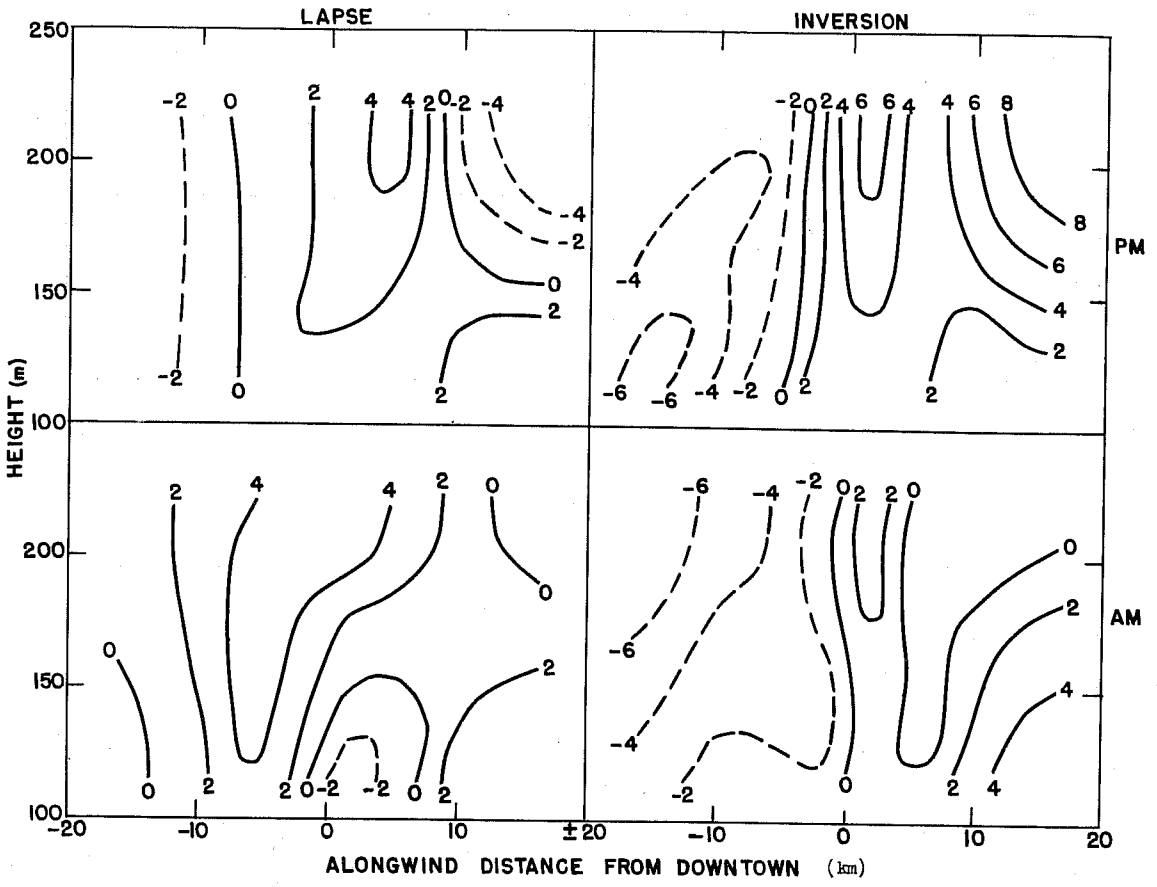

Figure 6. Vertical velocity (cm sec^{-1}) determined from tetroon flights across Columbus, Ohio, in lapse and inversion conditions before and after midnight. Positive numbers and solid lines indicate upward motion.

all cases; however, when the wind is strong a very different pattern results. Figure 7 shows the average nighttime vertical velocity in relation to city center when the wind was from the west at about 17 m sec^{-1} (top) and from the east at about 13 m sec^{-1} (bottom). In the former case the upward air motion near the city center amounts to 1 m sec^{-1}, and the city apparently induces damped vertical motions of opposite sense downwind of the city. A similar pattern is obtained with slightly lighter winds from the east. Under such windy conditions one might expect the city-induced vertical velocities to extend to considerable heights.

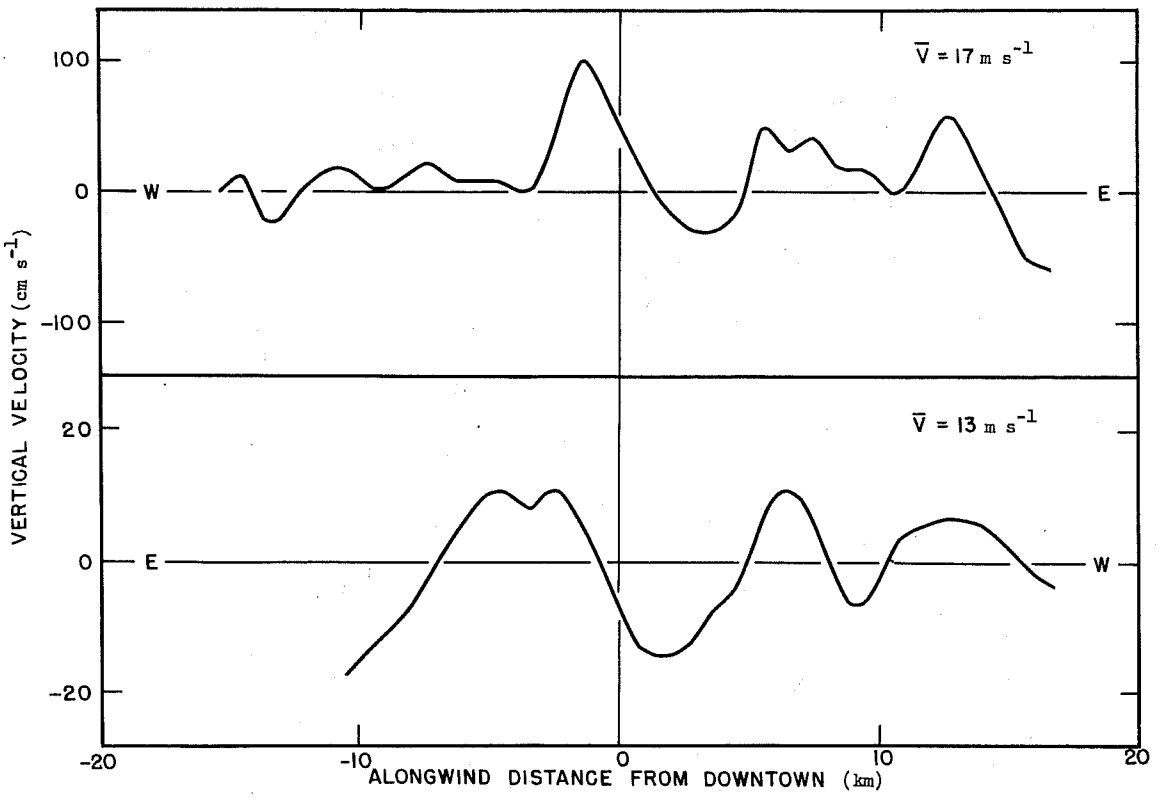

Figure 7. Average vertical velocity (cm sec^{-1}) determined from tetroon flights across Columbus, Ohio, on individual nights with strong winds from the west (top) and from the east (bottom). Note the five-fold difference in vertical velocity scale.

1.1.3 The Representativeness of Reynolds Stresses From Tetroon Flights

The tetroon flights past the BREN tower at the Nevada Test Site yield the first direct comparison between the vertical momentum flux derived from conventional fixed-point instrumentation and from tetroon flights. Figure 8 indicates the variation with local time of the fluxes obtained from fixed anemometers on the BREN tower (B), from the tetroon flights tracked by a radar near the base of the BREN tower (J), and from the tetroon flights tracked by a radar 15 km upwind from the tower (L). The difference in flux values obtained by the two radars suggests that there is considerable spatial variability in the flux in this area. Close to the tower, however, the tetroons appear to yield representative

flux values in the average for 5 days. Figure 9 shows the vertical momentum flux over Columbus, Ohio, obtained from tetroon flights across the city. In this case the eddy velocities represent deviations from 5-min average velocities. In most cases fluxes appear reasonable, with the maximum downward flux occurring slightly downwind of city center. Further work is planned on this important problem of the representativeness of tetroon-derived momentum fluxes.

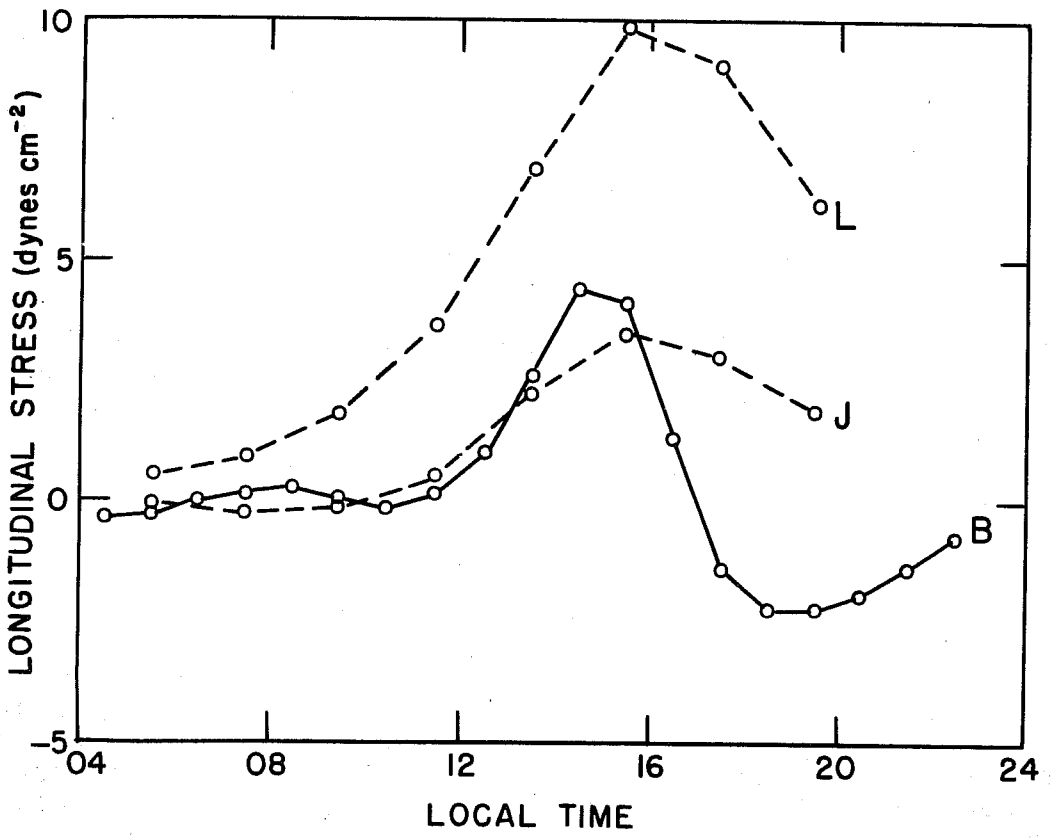

Figure 8. Average variation with local time of day of the longitudinal stress obtained by bivane at a height of 460 m on the BREN tower (B), and obtained from tetroon flights tracked by a radar close to the tower (J) and one 15 km to the southwest (L). An intervening mountain prevented simultaneous tracking of the tetroons by two radars.

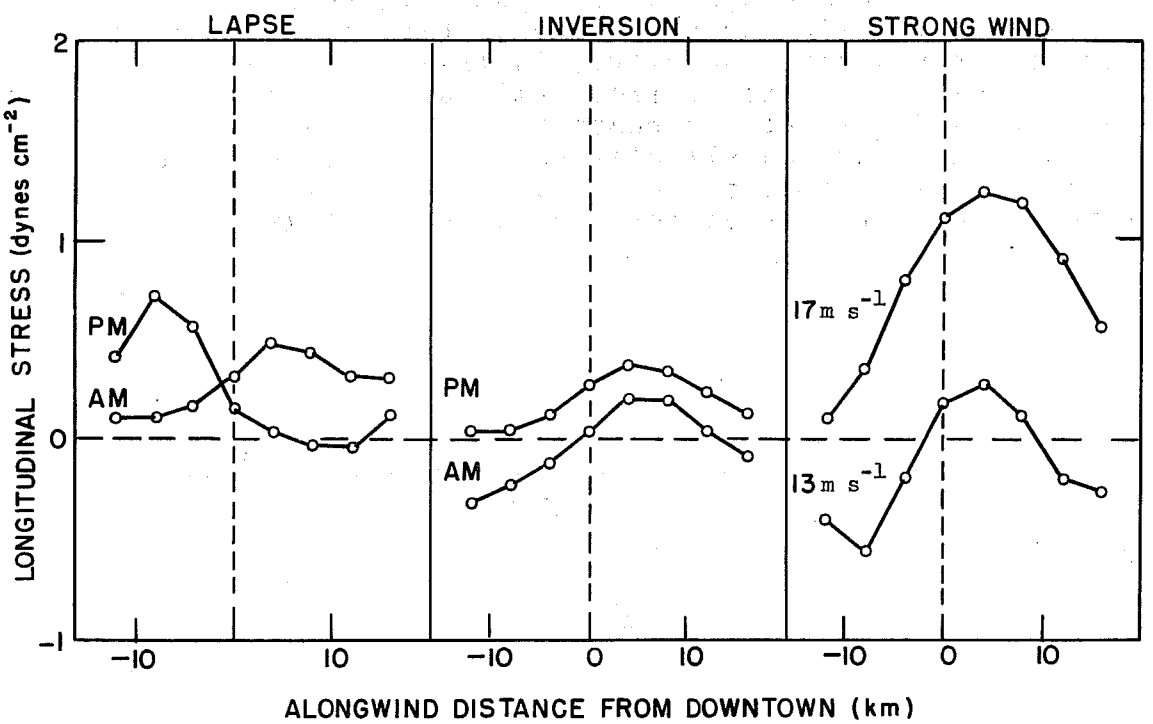

Figure 9. Variation of tetroon-derived longitudinal stress with upwind (negative abscissa) and downwind distance from Columbus, Ohio, in lapse and inversion conditions before and after midnight, and in relatively strong winds. Stress evaluations based on eddy velocities determined as the difference between 1-min and 5-min average tetroon velocities.

1.1.4 Urban Wind and Air Pollution Studies

Analysis of the tetroon data obtained in the Los Angeles Basin during September-October 1969 has awaited correction of tetroon positioning errors. In addition, it was desirable to obtain the terrain height in the basin before proceeding further. Such heights have now been obtained at ½ km intervals in computer compatible form and will be used to determine tetroon heights above the terrain. The method of estimating trajectories from winds at fixed locations (ERLTM-ARL 20) has applied to the surface wind network within the Los Angeles Basin, and work is commencing on the comparison of tetroon and surface trajectories. This will enable us to estimate the representativeness of the surface air flow for determining pollutant transport in the planetary boundary layer. This work will be completed within the next 6 months.

1.2 Mixing Length Hypotheses

The mixing length model described previously (ERLTM-ARL 9), when applied to the downwind flux of a scalar property S under horizontally uniform conditions, leads to an expression of the form

$$\overline{u'S'} = A\frac{\partial \bar{u}}{\partial z}\frac{\partial \bar{S}}{\partial z} + B\frac{\partial \bar{S}}{\partial z} . \qquad (1)$$

A series of 82 runs measured by a MIT research team at Round Hill, Mass., has been examined to determine the magnitude of the coefficients A and B when S represents temperature. Preliminary examination suggests that A ranges from approximately -2×10^3 m^2 in unstable conditions to approximately -2×10^2 m^2 in near-neutral and stable conditions, while B varies from about 10^2 m^2 sec^{-1} in unstable conditions to near 0 in neutral and stable conditions. However, the data show considerable scatter, which may be due in part to the surface features at Round Hill being such that the assumption of horizontal uniformity is questionable. Unfortunately horizontal gradients were not measured. A set of measurements taken under more ideal conditions in central Kansas will be examined in the same way; however, not as many runs are available at the Kansas site as are available at the Round Hill site. The investigation is continuing.

1.3 Planetary Boundary Layer Dynamics

An experiment was performed that will permit comparison of the mean winds measured at six levels on a 500-m tower with the mean wind distribution in the lowest 500 m of the atmosphere as determined by tracking a large number of pilot balloons serially released in the near the tower. This experiment was to establish whether the accuracy with which mean winds can be determined by tracking balloons with optical theodolites is comparable with that obtainable from fixed instruments mounted on a tower, and if so, what the optimum balloon ascent rate, frequency of release, frequency of positioning, etc., are likely to be. The ultimate application is for studies of planetary boundary layer dynamics, in which the mean wind distribution must be known to heights of about 2 km, far higher than the typical 300 to 500 m height of a tall tower.

The experiment was done during May and June 1970, using the 500-m WKY-TV tower in Oklahoma City, which has been instrumented by NOAA's National Severe Storms Laboratory. More than 600 wind soundings were taken, the typical procedure being to release a balloon every 3 min for a 90 min period and to track each balloon for 4 min. (Use of two tracking teams permitted soundings to "overlap" in time.) Of a total of 20 data periods, a majority appear to have at least 20 of the 30 soundings sufficiently "good," i.e., sufficiently free from missing or questionable observations, to produce a mean wind profile suitable for comparison with the tower data. In approximately one-third of the cases, the balloons were tracked by three theodolites rather than two, which permitted assessment of the variability due to only tracking procedure as well as that variability resulting from the failure of an individual balloon trajectory to adequately represent the mean flow in the atmosphere. These data are currently being analyzed.

2. RESEARCH AT THE NATIONAL REACTOR TESTING STATION, IDAHO

2.1 Mesoscale Transport Studies

2.1.1 Comparisons of Trajectories Derived From Wind Fields and Single Station Wind Data

One of the major reasons for studying the mesoscale temporal and spatial variability of the wind in the boundary layer is to investigate the reliability of the practice of assuming the wind data at the source may be applied over long distances in estimating the transport of an effluent. A series of trajectories of sequentially released hypothetical particles transported by the winds obtained from the mesoscale tower network has been presented and discussed (ERLTM-ARL-20, 1970). The method of constructing the trajectories and interpreting the trajectory plots has been presented in an earlier report (ERLTM-ARL-17). The plots presented showed that flow patterns do occur over the upper Snake River Plain which give rise to transport that would be very poorly represented by the assumption that source wind was representative of the flow over the whole area.

To provide a more graphic demonstration of this situation, several trajectory plots are presented in figures 10 and 11. The release location for this series of trajectories is the Power Burst Facility (PBF) located in the south central part of the NRTS. Each plot contains the trajectories of 12 "particles" released 1 hour apart beginning with the time at the top of each plot. The transport process is allowed to preceed for 12 hours after the release of the last "particle" or until all the particles are off the grid, whichever comes first. The upper row of plots, denoted by the letters WF (wind field), in each figure contains trajectories constructed from the wind data of the tower network. The lower row of plots, denoted by the letters SS (single station), contains trajectories for the same time period constructed under the assumption that the wind at the release point applied over the entire grid.

In figure 10, the cases with releases beginning at 1300 MST, 03/01/69 and 1300 MST, 04/03/69 demonstrate that the wind at the release point provides no indication of the eddy centered approximately 20 miles to the north-east. For the release beginning at 1300 MST, 03/04/69, the release point wind indicates a reversal from northwest to southeasterly flow and misses completely the transport to the northeast. For the release beginning at 0100 MST, 06/21/69, the release point winds transport the material about 20 miles farther to the northeast before the wind shifts.

In figure 11, for the release beginning at 0100 MST, 07/05/69, the release point wind causes a serious deflection of the transport as indicated by the wind field analyses. For the releases beginning at 1300 MST, 07/22/69; 1300 MST, 09/01/69; and 1300 MST, 09/03/69, the eddy to the northeast is not indicated by the release point winds.

These discrepancies in the flow patterns obtained by the two methods indicate that, at least for the situations presented here, the wind at the release point is not a reliable guide for determining transport for more than a few miles or a few hours. This is not to say that there are not times when the release point will be representative, because a number of the trajectory plots generated indicate a strong steady wind over the entire grid. The effect of this assumption on transport statistics is being investigated and is discussed briefly in section 2.1.4 of this report. Regardless of the effect on long-term statistics, however, the diagrams presented here demonstrate that on any given day, the application of the wind at the release point for more than a few miles or a few hours can result in serious errors in the estimation of effluent transport.

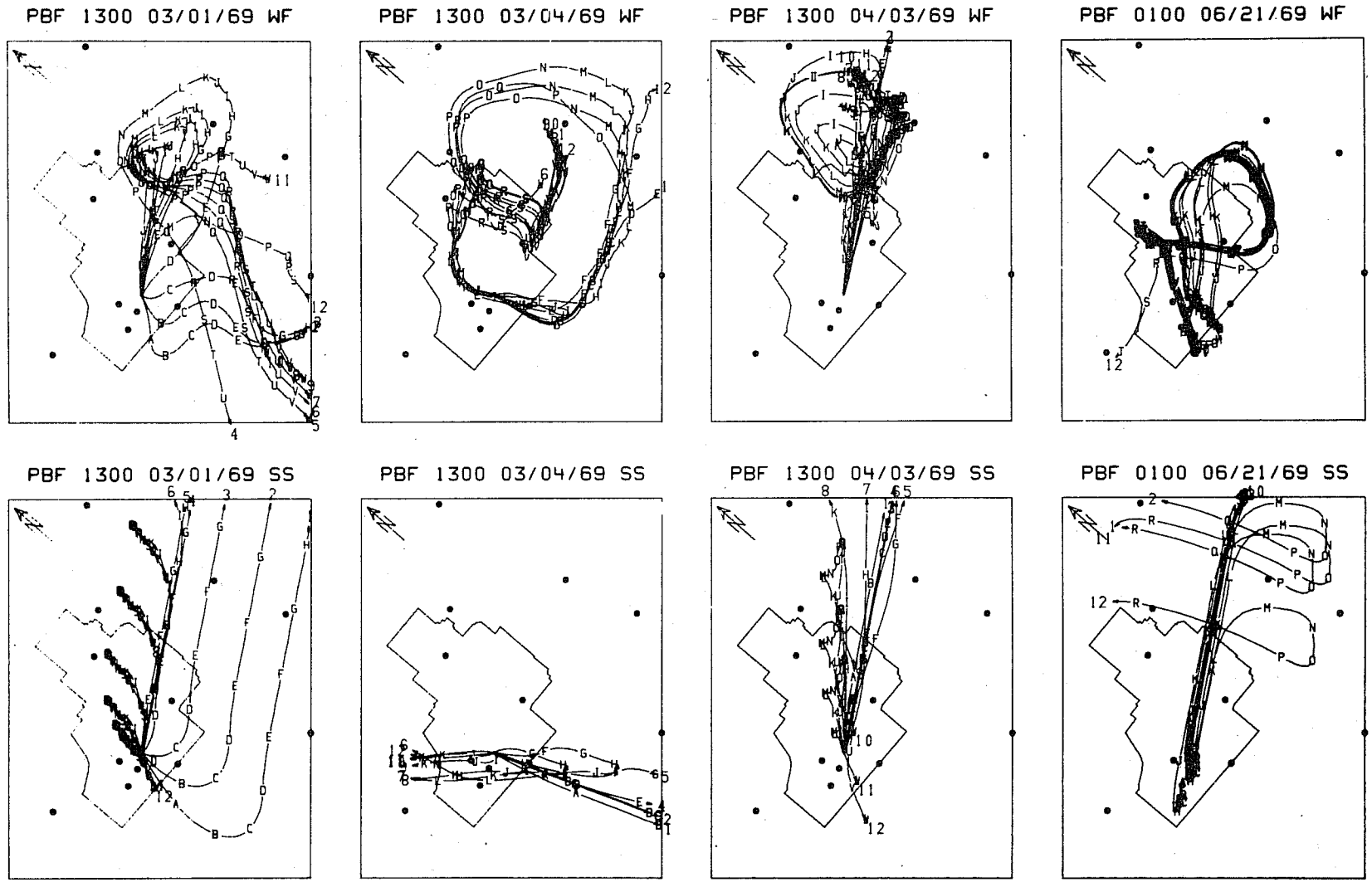

Figure 10. Trajectories of hypothetical particles released hourly. In upper plots (WF) the transporting velocity was provided by a time series of objectively interpolated wind fields. The transporting velocity for the lower plots was the wind at the release point. The letters along the trajectories indicate hourly positions. For scaling purposes the northern boundary of the site is 10.7 miles long.

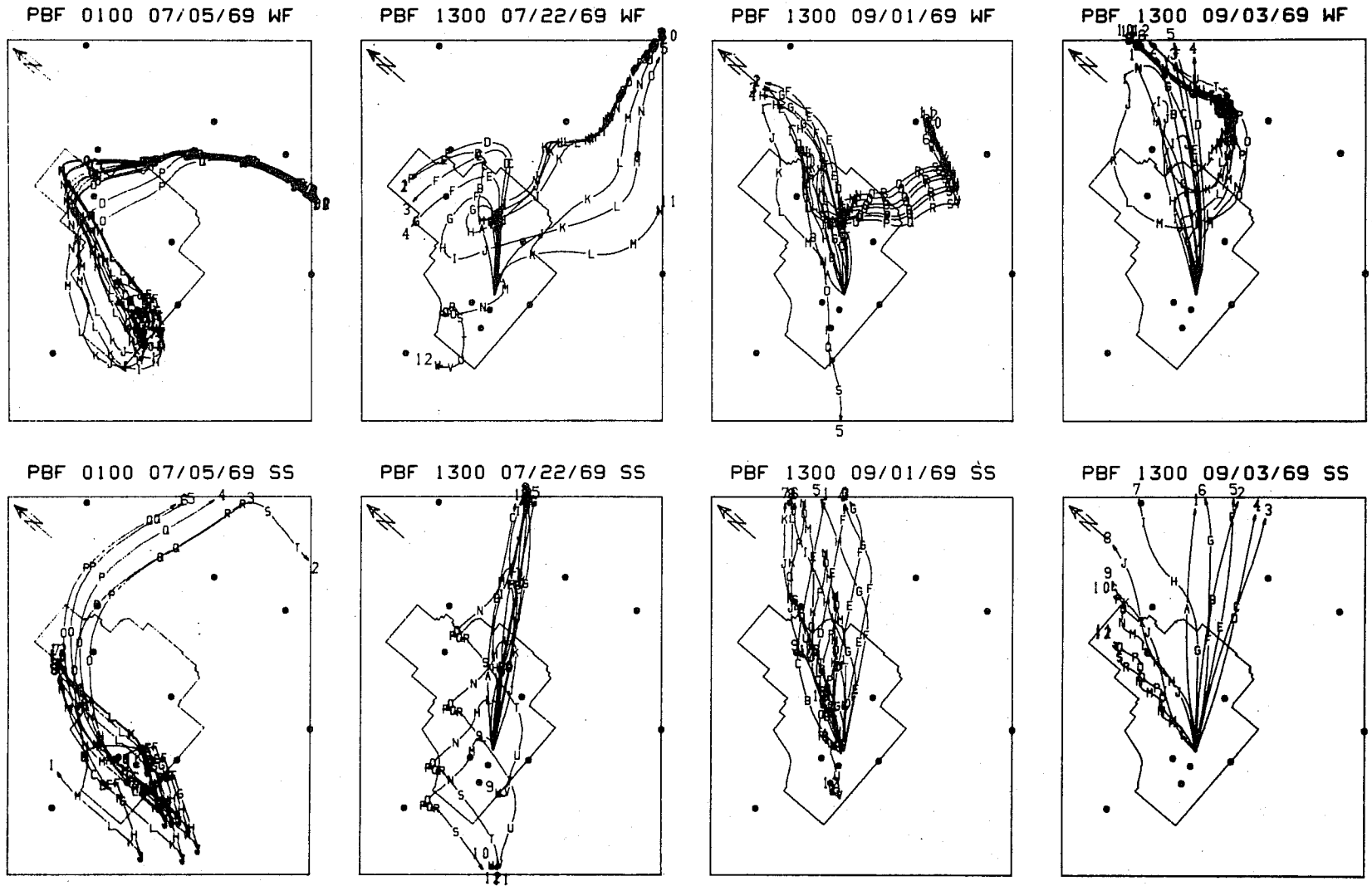

Figure 11. Trajectories of hypothetical particles. See figure 10 for details.

2.1.2 *Trajectory Statistics for Selected Receptors*

Since the method of interpolating wind fields on a regular grid using raw data from randomly spaced stations and the method of determining trajectories of hypothetical particles imbedded in these wind fields have been demonstrated (ERL-ARL 20, 1970), it has become possible to calculate various transport statistics from any point on the meso wind field grid to any other point on the grid. Presented here are certain transport statistics from one release point to a few selected population centers for the spring of 1969. This initial work is limited to one season, because it was performed at the request of the Operational Safety and Technical Support Division, USAEC, ID. Some of these transport statistics are already available for the other three seasons and from a good selection of release points for each season of the year. The project is continuing in order to obtain a greater variety of transport statistics based on larger samples.

The sample included 2184 trajectories, since one hypothetical particle is released every hour. Although the sample appears large enough, the term 'climatology' should not be used in referring to the results. Changes in the synoptic scale weather patterns, which in turn are the greatest single driving force upon the local winds, are measured in terms of days, and the 91 sample days are too few to establish a climatology. Even more significant is the synoptic scale weather systems having persistent abnormalities in their patterns due to the macro- or global-scale weather patterns, which in turn have changes measured in months and seasons. Nevertheless, the difference in transport statistics from 1 year to the next is not so great but what the study of a single year will give meaningful and useful results.

Two types of computations were made. The first was to record the number of occurrences of trajectories crossing any given area of concern. The computations were printed in a 24 x 12 matrix having the arguments 'hour of initial release,' and 'number of hours since release.' The latter argument resulted in only 12 columns since trajectories were followed for only 12 hours. Examples of the matrix for three population centers are shown in tables 1-3. Tabular entries are the number of occurrences in a 91-day (2184 hr) period. The times 0500-1900 MST and 2000-0400 MST closely approximate releases under lapse and inversion conditions in spring. The 0500 MST release is considered lapse, because even in early April lapse conditions will probably prevail by the time the trajectory reached any target.

Table 1. Occurrences of Trajectory Crossings Over Arco, Idaho, From April 1 to June 30, 1969.

Hour of Release	Number of Hours Since Release[1]												
	1	2	3	4	5	6	7	8	9	10	11	12	SUMS
1	0	0	0	0	0	0	0	1	0	0	0	0	1
2	0	0	0	0	0	0	1	0	0	0	0	0	1
3	0	0	0	0	0	1	1	0	0	0	0	0	2
4	0	0	0	0	0	0	0	1	0	0	0	0	1
5	0	0	0	1	1	0	1	0	0	0	0	1	4
6	0	0	1	0	1	1	0	0	0	0	1	0	4
7	0	0	0	2	0	0	0	0	0	0	1	0	3
8	0	0	0	0	0	0	0	0	0	0	0	0	0
9	0	0	0	0	0	0	0	0	0	0	0	0	0
10	0	0	0	0	0	0	0	0	0	0	0	0	0
11	0	0	0	0	0	1	0	0	0	0	0	0	1
12	0	0	0	0	0	0	0	0	0	0	0	0	0
13	0	0	0	0	0	0	0	0	0	0	0	0	0
14	0	0	0	0	0	0	0	0	0	0	0	0	0
15	0	0	0	0	0	0	0	0	0	0	0	0	0
16	0	0	0	0	0	0	0	1	0	1	0	0	2
17	0	0	0	0	0	0	0	0	0	0	0	0	0
18	0	0	0	0	0	0	0	0	0	0	0	0	0
19	0	0	1	0	0	0	0	0	1	0	0	0	2
20	0	0	0	0	0	0	0	0	0	0	0	0	0
21	0	0	0	0	0	1	0	0	0	0	0	0	1
22	0	0	0	0	0	0	1	0	0	0	0	0	1
23	0	0	0	0	0	0	0	0	0	0	0	0	0
24	0	0	0	0	0	0	0	0	0	1	0	0	1
SUMS	0	0	2	3	2	4	4	3	1	2	2	1	24

Table 2. Occurrences of Trajectory Crossings Over Mud Lake, Idaho, From April 1 to June 30, 1969.

Hour of Release	Number of Hours Since Release[1]												
	1	2	3	4	5	6	7	8	9	10	11	12	SUMS
1	0	8	2	1	1	2	1	0	0	1	0	0	16
2	0	7	6	1	0	2	1	0	1	0	0	0	18
3	0	10	4	2	1	2	0	1	0	0	2	1	23
4	0	10	1	4	1	1	1	0	0	1	0	0	19
5	0	11	1	4	1	1	0	0	1	0	0	0	19
6	0	6	4	1	0	1	0	1	0	0	0	0	13
7	0	2	2	0	1	2	1	0	1	1	0	0	10
8	0	3	0	2	0	1	1	0	0	1	0	1	9
9	0	1	1	1	3	1	0	1	1	1	1	0	11
10	0	1	2	0	0	2	3	0	0	0	0	0	8
11	0	1	1	1	4	0	0	1	1	0	0	0	9
12	0	1	0	3	0	0	1	2	0	1	0	1	9
13	0	1	0	0	0	2	1	0	0	0	1	1	6
14	0	1	2	0	1	0	1	1	0	2	1	1	10
15	0	1	3	2	0	0	0	2	1	1	0	0	10
16	0	0	0	1	1	2	0	1	0	2	1	1	9
17	0	0	0	1	1	2	1	1	1	1	0	0	8
18	0	1	1	1	1	2	0	2	2	1	1	0	12
19	0	0	1	1	1	3	3	3	0	2	0	0	14
20	0	0	1	4	1	2	2	1	2	0	0	0	13
21	0	1	4	1	4	2	0	1	0	0	0	0	13
22	0	3	3	5	2	0	1	0	0	0	0	0	14
23	0	3	5	1	0	1	1	0	1	0	0	0	12
24	0	5	3	2	1	1	0	1	0	0	0	0	13
SUMS	0	77	47	39	25	32	19	19	12	15	7	6	298

[1] For hourly releases from PBF as a function of initial hour of release and hour since release

Table 3. Occurrences of Trajectory Crossings Over Idaho Falls, Idaho, From April 1 to June 30, 1969.

Hour of Release	Number of Hours Since Release[1]												
	1	2	3	4	5	6	7	8	9	10	11	12	SUMS
1	0	0	0	0	1	1	0	0	1	0	0	0	3
2	0	0	0	1	0	1	0	0	0	0	0	0	2
3	0	0	1	1	0	0	1	0	0	0	1	0	4
4	0	0	1	1	1	2	0	0	0	1	0	0	6
5	0	0	1	1	1	0	0	0	1	0	0	0	4
6	0	0	0	0	0	0	0	0	0	2	0	0	2
7	0	0	0	0	0	0	0	0	0	0	1	0	1
8	0	0	0	0	0	0	1	0	0	1	0	0	2
9	0	0	0	0	1	1	0	0	0	0	0	0	2
10	0	0	0	0	1	0	0	1	0	1	0	0	3
11	0	0	0	1	0	0	0	0	1	1	0	0	3
12	0	0	0	0	0	0	0	0	0	0	0	1	1
13	0	0	0	0	0	0	2	0	0	0	1	0	3
14	0	0	0	0	0	2	0	1	0	1	0	0	4
15	0	0	0	0	0	0	1	1	0	0	0	0	2
16	0	0	0	0	0	1	0	0	0	0	0	0	1
17	0	0	0	0	0	0	0	0	0	0	0	0	0
18	0	0	0	0	0	0	0	0	0	0	1	1	2
19	0	0	0	0	0	1	0	0	0	1	0	1	3
20	0	0	0	0	0	0	0	0	0	1	1	0	2
21	0	0	0	0	0	0	0	0	0	1	0	0	1
22	0	0	0	0	0	0	0	0	1	0	2	0	3
23	0	0	0	0	1	0	1	1	0	2	0	0	5
24	0	0	0	0	0	2	0	1	0	0	0	0	3
SUMS	0	0	3	5	6	11	6	5	4	12	7	3	62

[1] For hourly releases from PBF as a function of initial hour of release and hour since release

The second type of computation was the number of occurrences of classes of 'dwell time' of the hypothetical particles over the area. The time of dwell began when a trajectory reached the area and no other trajectory was over the area the previous time period. The time of dwell ended when no trajectory is again found over the area. The dwell time may be either the result of a stream of trajectories passing over the area with a steady wind, or the result of one or more trajectories stagnating over the area with light and variable winds. The occurrences were printed in a 24 x 20 matrix having the arguments 'hour of initial crossing,' and 'hours of dwell.' Trajectories were followed for 20 hours to compute dwell time. Examples of the second matrix for three population centers are shown in tables 4-6 for a 24 x 12 matrix size, since the longest dwell time was found to be 12 hours. The release point for the trajectories is the Power Burst Facility (PBF) located slightly less than 1 km from the SPERT wind station shown in figure 12. This figure also shows the circle of

Table 4. Occurrences of Total Collective Dwell Times Over Arco, Idaho, From April 1 to June 30, 1969.

Hour of Crossing	Number of Hours Total Dwell[1]											
	1	2	3	4	5	6	7	8	9	10	11	12
1	0	0	0	0	0	0	0	0	0	0	0	0
2	1	0	0	0	0	0	0	0	0	0	0	0
3	2	0	0	0	0	0	0	0	0	0	0	0
4	2	0	0	0	0	0	0	0	0	0	0	0
5	0	0	0	0	0	0	0	0	0	0	0	0
6	0	0	0	0	0	0	0	0	0	0	0	0
7	0	0	0	0	0	0	0	0	0	0	0	0
8	1	0	0	0	0	0	0	0	0	0	0	0
9	2	0	0	0	0	0	0	0	0	0	0	0
10	3	0	0	0	0	0	0	0	0	0	0	0
11	1	1	0	0	0	0	0	0	0	0	0	0
12	0	0	0	0	0	0	0	0	0	0	0	0
13	0	0	0	0	0	0	0	0	0	0	0	0
14	0	0	0	0	0	0	0	0	0	0	0	0
15	0	0	0	0	0	0	0	0	0	0	0	0
16	1	0	0	0	0	0	0	0	0	0	0	0
17	0	1	0	0	0	0	0	0	0	0	0	0
18	0	0	0	0	0	0	0	0	0	0	0	0
19	0	0	0	0	0	0	0	0	0	0	0	0
20	0	0	0	0	0	0	0	0	0	0	0	0
21	0	0	0	0	0	0	0	0	0	0	0	0
22	1	0	0	0	0	0	0	0	0	0	0	0
23	0	0	0	0	0	0	0	0	0	0	0	0
24	1	0	0	0	0	0	0	0	0	0	0	0
SUMS	15	2	0	0	0	0	0	0	0	0	0	0

Table 5. Occurrences of Total Collective Dwell Times Over Mud Lake, Idaho, From April 1 to June 30, 1969.

Hour of Crossing	Number of Hours Total Dwell[1]											
	1	2	3	4	5	6	7	8	9	10	11	12
1	2	1	0	0	0	0	0	0	0	0	0	0
2	6	2	0	0	0	0	0	0	0	0	0	0
3	8	1	1	0	0	0	0	0	0	0	0	0
4	9	2	2	0	0	0	0	0	0	0	0	0
5	10	0	2	0	0	0	0	0	0	0	0	0
6	11	0	1	1	1	0	0	0	0	0	0	0
7	12	2	1	0	0	0	0	0	0	0	0	0
8	9	3	0	0	0	0	0	0	0	0	0	0
9	5	3	1	0	0	0	0	0	0	0	0	0
10	3	3	2	0	0	0	0	0	0	0	0	0
11	1	0	0	0	0	0	1	0	0	0	0	0
12	2	1	1	0	0	0	0	0	0	0	0	0
13	5	0	0	1	0	0	0	0	0	0	0	0
14	2	0	1	0	0	0	0	0	0	0	0	1
15	2	0	0	0	0	1	0	0	1	0	0	0
16	0	1	0	1	0	0	0	0	0	0	0	0
17	1	0	3	0	0	0	0	0	0	0	0	0
18	0	1	0	1	0	0	1	0	0	0	0	0
19	1	0	1	0	0	0	0	0	0	0	0	0
20	2	0	1	0	1	0	0	0	0	0	0	0
21	1	2	1	0	0	0	0	0	0	0	0	0
22	1	0	1	0	1	1	0	0	0	0	0	0
23	1	3	0	1	0	0	0	0	0	0	0	0
24	5	0	0	2	0	0	0	0	0	0	0	0
SUMS	99	25	19	7	3	2	2	0	1	0	0	1

[1] For hourly releases from PBF as a function of hour of initial crossing and the number of hours of dwell time

Table 6. Occurrences of Total Collective Dwell Times Over Idaho Falls, Idaho, From April 1 to June 30, 1969.

Hour of Crossing	Number of Hours Total Dwell[1]											
	1	2	3	4	5	6	7	8	9	10	11	12
1	1	0	0	0	0	0	0	0	0	0	0	0
2	0	0	0	0	0	0	0	0	0	0	0	0
3	0	0	0	0	0	0	0	0	0	0	0	0
4	0	1	0	0	0	0	0	0	0	0	0	0
5	0	0	0	1	0	0	0	0	0	0	0	0
6	0	0	2	0	0	0	0	0	0	0	0	0
7	3	1	0	0	0	0	0	0	0	0	0	0
8	0	2	0	0	0	0	0	0	0	0	0	0
9	3	0	0	0	0	0	0	0	0	0	0	0
10	1	0	0	1	0	0	0	0	0	0	0	0
11	1	0	0	0	0	0	0	0	0	0	0	0
12	0	0	0	0	0	0	0	0	0	0	0	0
13	1	0	0	0	1	0	0	0	0	0	0	0
14	0	1	0	0	0	0	0	0	0	0	0	0
15	0	0	0	0	0	0	0	0	0	0	0	0
16	1	0	1	0	0	0	0	0	0	0	0	0
17	1	1	0	0	0	0	0	0	0	0	0	0
18	0	1	0	0	0	0	0	0	0	0	0	0
19	1	0	0	0	0	0	0	0	0	0	0	0
20	1	0	1	1	0	0	0	0	0	0	0	0
21	0	1	0	0	0	0	1	0	0	0	0	0
22	1	0	1	0	0	0	0	0	0	0	0	0
23	0	1	0	0	0	0	0	0	0	0	0	0
24	0	1	0	0	0	0	0	0	0	0	0	0
SUMS	15	10	5	3	1	0	1	0	0	0	0	0

[1] For hourly releases from PBF as a function of hour of initial crossing and the number of hours of dwell time

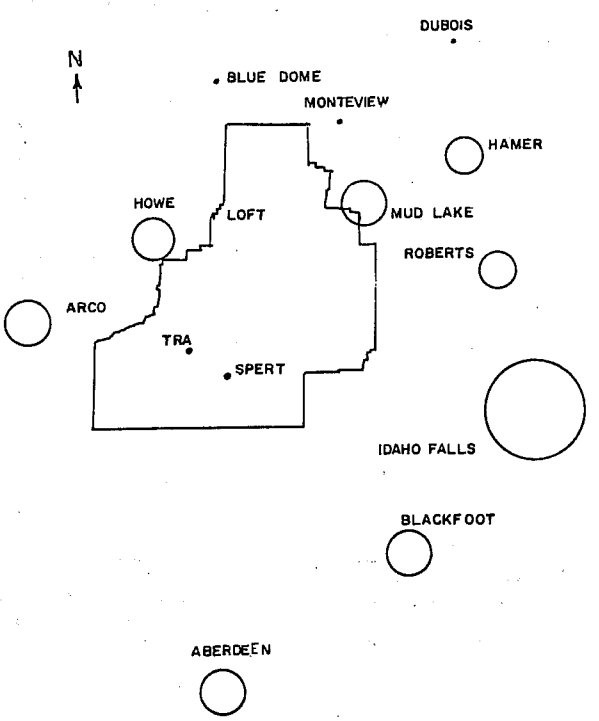

Figure 12. Locations and radii of concern for the population centers for which transport statistics are computed.

concern around a number of population centers. If a trajectory touches or comes within this circle the trajectory is considered to have crossed the population center. Table 7 shows the distance of the radius of concern around the various population centers and the distance from PBF.

These statistics revealed facts that cannot be determined from a wind rose. The hourly wind roses for the Central Facilities Area (CFA) indicate a distinct maximum of SW winds in the afternoon in spring, so who would have anticipated that Mud Lake, which is downstream from PBF under SW wind flow, would have experienced a maximum of crossings from trajectories released at night rather than during the day? Yet this is what is shown in table 8. The number of trajectory crossings is far greater at Arco than would have been estimated from the CFA wind rose, which shows an extremely low probability of getting the proper sequence of NE-E and SE winds. The value of these transport statistics gives a distinctly additional order of approximation to the true transport statistics when compared with previous methods giving only a rudimentary first approximation.

Table 7. Population Centers for Which Transport Statistics Were Computed.

Population Center	From PBF (km)	Radius of Concern (km)	Trajectory Hits (WF[1])	(SS[2])
Arco	39.3	3.4	24	4
Howe	27.8	3.4	49	70
Monteview	56.8	3.4	117	81
Mud Lake	43.0	5.1	298	243
Hamer	63.8	3.4	65	108
Roberts	57.5	3.4	52	41
Idaho Falls	60.8	9.4	62	46
Blackfoot	51.6	5.1	13	9
Aberdeen	62.3	3.4	6	10

[1] Interpolated wind fields
[2] Single station analysis of wind fields

Table 8. The Percentage of Days That One or More Trajectory Hits Were Recorded at the Population Centers.

Population Center	24-hour (%)	Days[1]	
		0500-1900 MST	2000-0400 MST
Arco	14	11	6
Howe	22	12	15
Monteview	38	25	26
Mud Lake	58	41	51
Hamer	28	16	15
Roberts	23	15	11
Idaho Falls	22	14	12
Blackfoot	8	4	4
Aberdeen	7	3	3

[1] Days are counted according to release times from PBF

A second test was conducted to examine the relation of frequency of trajectory crossings to size of radius of concern. The test was performed on a station near the periphery of the grid, namely Arco, as opposed to a station near the center of the grid and in the mainstream of trajectories riding the prevailing SW winds, such as at Mud Lake. The results for radius sizes 0.1 through 2.0 grid units (0.5 through 10.7 miles) is shown in figure 13. Remember that there is a degree of uncertainty in the determination of the trajectories because of vertical wind shear. Because of this uncertainty, one would use varying radii of concern in safety analysis according to the risk that can be taken.

A third test was conducted to determine the effect on the transport statistics by using single station wind analysis to determine the trajectories instead of a wind field interpolated from 21 wind stations to determine the trajectories, which were computed using only the winds at the release point. The resulting trajectory crossings are compared with those obtained from interpolated wind fields and are shown

as part of table 7. A drastic effect was noted at Arco where only four trajectories crossed the target area. At Mud Lake there was a reduction to 243 trajectory crossings, which appears to be due only to a slightly different characteristic pattern of the trajectories. Monteview also had a reduction, but Howe and Hamer had significant increases. Idaho Falls fell to 46 crossings with the trajectories determined by single station (SS) winds. The immediate conclusion is that the two sets of transport statistics are different enough to merit the use of wind fields (WF) determined by many wind stations in determining trajectories. The results of these experiments, preliminary though they are, indicate that where organized and repetitive mesoscale circulations exist (examples are sea breezes and mountain-valley winds) the sequential time-space behavior of the wind field may yield exposure or dosage probabilities that differ markedly in location and value from statistics obtained from a single, source-located wind measurement.

2.1.3 Error Checking and Correction

The handling of the meso-network wind data between the time the ink dries on the strip chart and the time that numerical values are stored on a magnetic tape or disc introduces

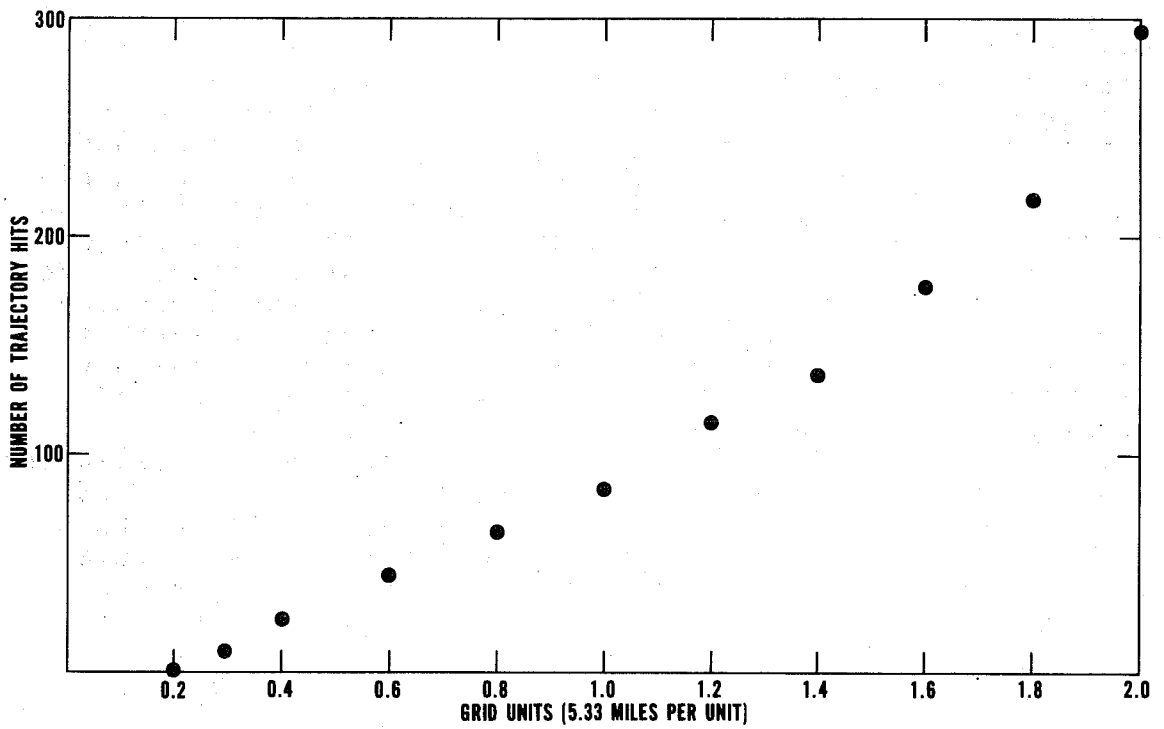

Figure 13. Number of trajectory hits at Arco by size of radius of concern in releases from PBF, spring 1969.

errors of various types. An attempt to uncover some of the more flagrant of these errors is made by subjecting the data to some automated error checking. The first test checks all the stations for wind speeds greater than 22.3 m sec^{-1}. The station name, speed, direction, and time of occurrence are printed out for use in checking the punch cards and the data forms. For all the stations, the data for 1969 had 57 distinct occurrences of hourly average winds of 22.3 m sec^{-1} or greater. Fourteen of these cases, however, resulted from illegible figures, keypunch errors, and recording errors. Every one of these errors resulted in a gross distortion of the data, and they were corrected in the stored information.

Another extremely important type of error encountered in the data resulted from the incorrect direction orientation of some of the wind vanes. Whether the cause of this problem was electronic, mechanical, human, or a combination of all three was not determined, but occasionally an orientation check at each station would uncover varying degrees of error at several of the stations. Because there was no way to determine when the orientation had changed since it was last checked, a scheme was devised to test the orientation of the stations from the data they had reported.

The test is based on the premise that under relatively strong wind conditions (greater than 6.7 m sec^{-1}) stations that are fairly close together should be reporting less than a 30° spread in their wind direction. This allows for a ±15° tolerance for the subjective averaging of the strip chart data. Six groups of four stations each were selected for this type of checking. For each hour, during which all four stations reported a wind greater than 6.7 m sec^{-1}, an average wind direction was computed, which was then recomputed not including the station that had the largest deviation from the average. The deviation was then recomputed for all four stations. The station names, the three-station average speed and direction, the recorded hourly average direction and speed for each station, and the deviations from the three-station average were then printed out for examination. The monthly averages of the deviations were also printed out. Generally if an orientation error persisted through a month, the average deviation was quite representative of the amount of correction needed as determined from an actual orientation check. The printout of the individual hourly results proved valuable in discovering a station where an orientation error occurred only when the wind had a direction from south through west. This indicated faulty equipment.

This technique has the disadvantage of requiring strong winds at all four stations. During a month that has only a few hours meeting this requirement, it would be risky to use

the results to correct the directions at a station for the whole month. Before corrections were made they were checked against maintenance records on some of the strip charts. The corrections to the wind direction data for 1969 are shown in table 9. These corrections were added algebraically to the original wind direction data.

2.1.4 Comparison of Tetroon and Wind Field Trajectories

One of the most pressing questions about trajectories computed from a tower or a surface network of wind stations is how well do they represent the transport of an actual effluent by the atmosphere in the boundary layer? We see from the trajectory plots of figures 14 and 15 that trajectories constructed from wind data from a network of stations should be more representative than trajectories constructed from a single station, but we cannot say quantitatively how close these trajectories are to actual trajectories. If the wind profile in the boundary layer consistently conformed to the Eckman spiral or logarithmic distribution, one might infer that, under conditions of thermal stability, the trajectories of the hypothetical particles could be constructed which would be quite representative. However, the boundary layer profile has been observed on occasion at several locations to show radical departures from these simple models. Thus determining the representativeness of the constructed trajectories presents a complex problem.

A seemingly simple approach to the verification of the wind field trajectories is to compare them with trajectories of tetroons ballasted to fly at altitudes of the tower wind measurements. The phrase "seemingly simple" is used because of the difficulty of keeping the tetroon in the desired height for more than a few hours. At the low altitude, occasionally the tetroon dips low enough to drag the instrument package through the sagebrush and eventually it becomes snagged. Another problem lies in the radar determination of the tetroon height above the terrain. To track the tetroons for any appreciable distance at low altitude, the tracking radar is located on a butte some 1500 ft above the surrounding terrain. This means that tracking at night involves the possibility of refraction as the radar signals pass through a temperature inversion. Also at long distances a very small error in a vertical angle reading can cause an error of several hundred feet in the computed elevation of the tetroon. With all the problems involved, however, the radar-tetroon-transponder system provides the most convenient and unique system for obtaining estimates of actual trajectories in the boundary layer.

Table 9. Direction Corrections† for Orientation Errors

Station Time (MST)	Date (1969)	CFA 250'	IET 150'	GRD3	EBR2 240'	NRF	SPRT	EBR1	ARCO	BSRN	TABR	KID	BLKF	ABDN	BLDM	DBS	MTV	RBRT	SDN	KTB
0100	01/01																			
2400	01/05	-50					30					10					10			
2300	01/06	-50					30	-150				10					10			
1800	01/21	-50					30					10					10			
2400	01/31	-50										10					10			
1200	02/04	-50															10			
0100	03/01																10			
0100	04/01				-30												10			
0100	05/01			20*	-20		10										10			
1000	05/09			20*	-20		10										10			-10
0100	07/01			20*	30		10				10						10			-10
1000	09/20			20*	30						10	10					10		-10	-10
2400	09/30			20*	20		70				10	10					10		-10	-10
1200	10/02				20		70				10	10					10		-10	-10
2400	10/31						70			40	10	10					10	10		-10
1200	11/05					50	70			40										
1600	12/05					50	70													
2400	12/31					50														

† Corrections are in degrees and apply from the previous date-time group to the date-time group directly on the left

* Correction in southwest quadrant only

Work has begun, during this reporting period, in which tetroon trajectories, which were obtained since the initiation of mesoscale wind tower network, are used in conjunction with the tower data to provide a comparison of these two types of trajectories. For preliminary examination, trajectories constructed from the wind field data were initiated at the same release times and locations of several tetroon releases. Computer plots of each pair of trajectories were produced for visual examination and separation distances were computed at half-hour intervals. Because more detailed work in this area is in progress, only the plots are presented and discussed briefly in this report.

In figure 14 the tetroon trajectories are shown with lower case letters appearing at 30-min intervals along the trajectories. The corresponding trajectories constructed from the wind field data are shown with upper case letters at the same intervals. The release times and dates for each trajectory are shown at the top of the individual plots. The releases in figure 14 were made a little less than an hour apart on the afternoon of November 17, 1969. Since part of the time that all three tetroons were in the air, position readings were staggered such that the interval between position fixes was 5 min for each tetroon. The wind was from the northwest to the north-northwest at about 10 to 12 mph. The computed wind field trajectories for the 1428 MST release time followed the tetroon trajectories quite closely with a maximum separation of about 2 miles at the end of the first half-hour. The trajectories released at 1516 MST show the tetroon moving about 50 percent faster than the wind field trajectory the first 1.5 hours, then slowing to about half the speed of the wind field trajectory during the last hour and one-half that it was tracked. The trajectories released at 1609 MST show a marked discrepancy in direction during the first half-hour of flight. This could be caused by a large change in altitude during this time. The tetroon release elevation was indicated to be 4900 ft MSL. It climbed to 11,600 ft MSL during the first 15 min of flight then dropped to 7200 ft MSL during the next 15 min. It continued down to an average elevation of 5100 ft MSL for the remainder of the flight during which the direction and speed were quite comparable to the computed one.

In figure 15 trajectories are shown for four releases during the afternoon and evening of December 1, 1969. The winds, with the exception of the valley breeze depicted by the trajectories released at 1722 MST, were very light. The tetroon released at 1446 MST simply drifted back and forth in an area with a 10 mile diameter for the entire 6.5 hours that it was followed. The hypothetical particle did the same for about 4 hours before it began to move slowly to the

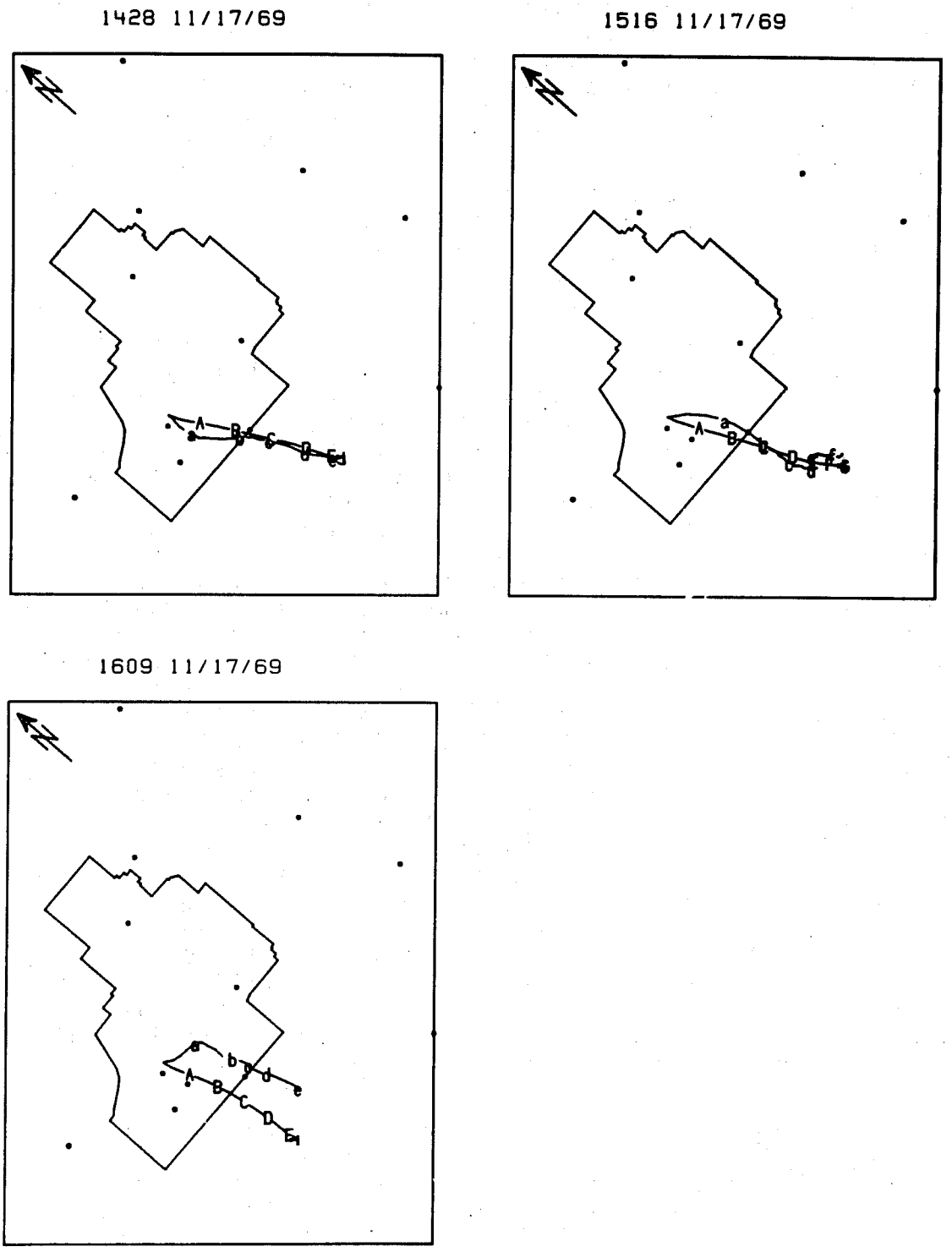

Figure 14. Trajectories of tetroons and hypothetical particles. For the tetroon trajectories lower case letters are used to indicate 30 min "particle positions."

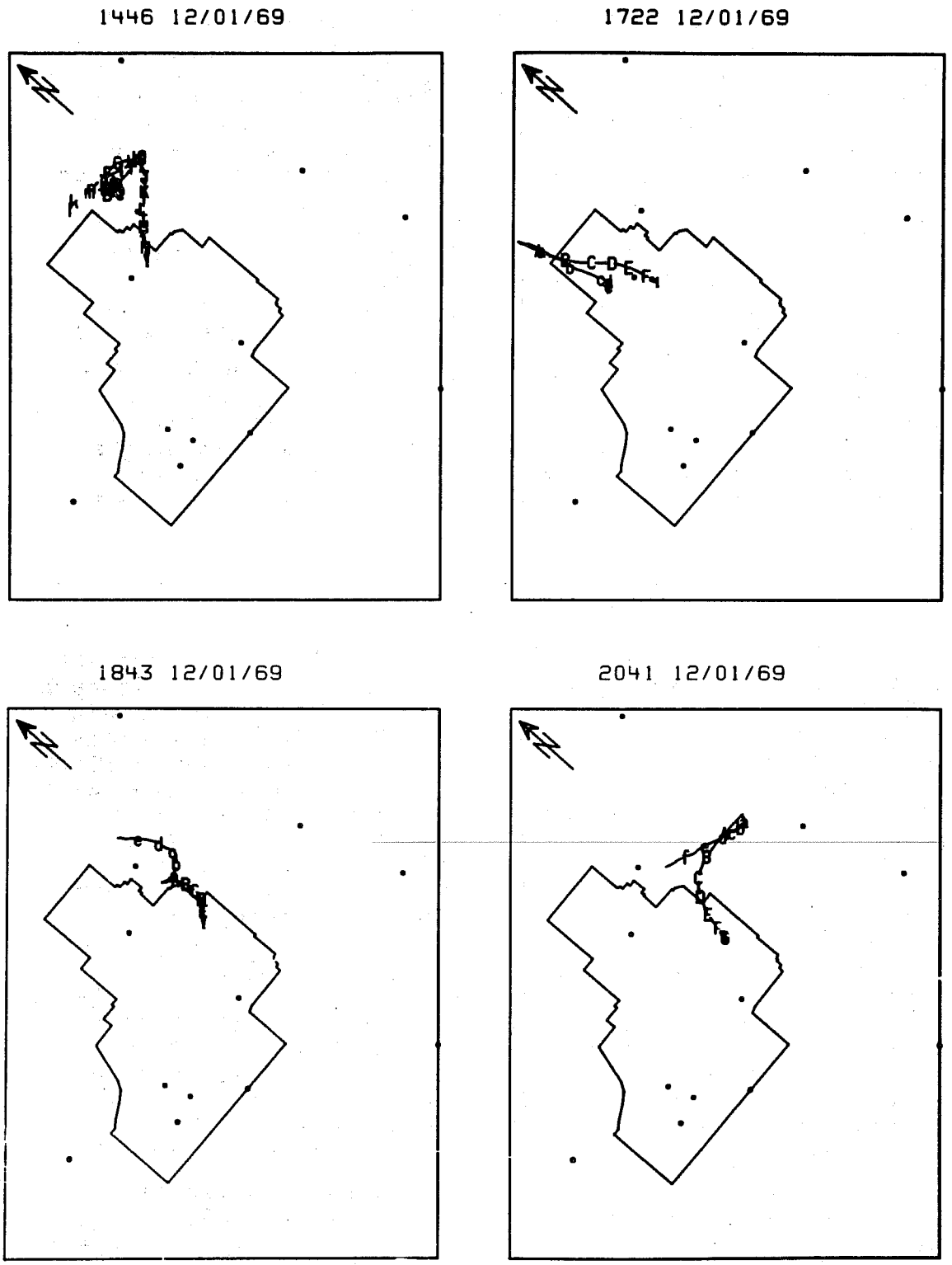

Figure 15. Trajectories of tetroons and hypothetical particles. See figure 14 for details.

southwest. The tetroon released at 1722 MST was released in a valley. It stayed quite close to the wind field trajectory until it dropped too low and became tangled in the sagebrush. The largest deviation of the eight cases presented here is shown by the last two releases in figure 15. They were both released well after dark and the heights indicated by the radar either were right at the surface or were below the surface. The tower winds used to obtain the "particle trajectory" were measured 100 to 150 ft above the ground. It is conceivable that the tetroons spent a good part of the time in a flow regime that the tower winds were too high to represent, but a more careful examination of all available data must be made before any concrete conclusions can be reached.

These few cases indicate that there are times when the tower winds will represent transport of real material, but situations also exist in which the vertical variations in speed and direction are too great to be represented by the measurements at one level. It will take more extensive experimentation and analysis to establish a clear picture of the physical situation.

2.1.5 Animation of Trajectory Plots

The type of trajectory plots shown in figures 14 and 15 show transport over a 24 hour period in one diagram. Although this type presentation has advantages, it requires a certain amount of effort on the part of an observer to deduce the details of the "particle" movement for any selected time period. For this reason the computer program that produces trajectory plots has been modified to produce a motion picture of the movement of "particles" released into the mesoscale wind field over the upper Snake River Plain. The particles are represented with consecutive upper case letters that appear at the source and then move as they are carried by the wind. As the letters leave the grid they change to dots, which remain at the exit points of the boundary. To keep a series of 24 letters distinguishable from the next series of 24 letters, the case of any letter that remains on the grid for more than 24 hours is changed from upper to lower. Motion pictures have been produced for two different release points for up to 72 hours from release time. This type of presentation is impressive because it is more dynamic and easier to interpret than a single plot containing the paths of several particles.

In an attempt to compare the two types of presentation a collection of movie frames are shown in figure 16. These frames are separated by 3 hours. On the movie film there are 48 frames $hour^{-1}$. The first nine frames depict the same "particle" transport as does the WF plot for a release

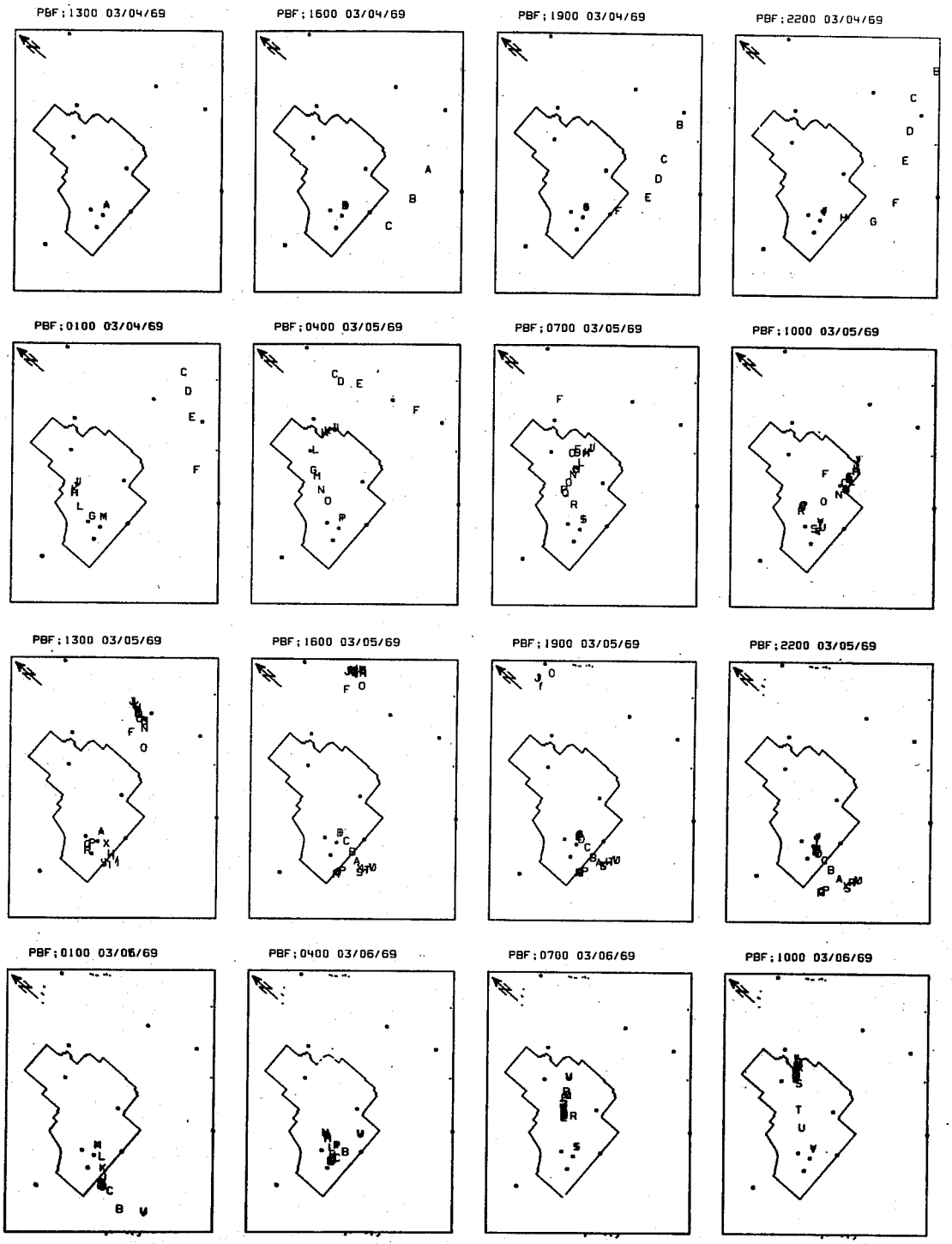

Figure 16. A series of selected movie frames showing position of "particles" released once an hour and transported by interpolated tower winds. Each is denoted by a letter.

beginning at 1300 MST 03/04/69 of figure 14. The only difference is that in the trajectory plot the release ends after 12 "particles" have been released, whereas "particles" in the animated version are released once an hour throughout the entire period of interest.

The details of the "particle" movement become clear much more easily from what is seen in the movie frames. For example, the divergence in the flow pattern that occurs at the southern end of the site between 2200 MST 03/05/69 and 0100 MST 03/06/69 is apparent from the separation of the "particle" marked F and G. The convergence in the northeast portion of the site between 0100 and 0700 MST 03/06/69 may be deduced from the merging of the group of particles marked C, D, and E with the group marked H, I, J, and K. Both of these groups and some of the "particles," which were subsequently released, form a crude line and sweep southward over the eastern portion of the site. This sequence of events is, of course, much more dynamic when observed in motion picture form than by observation of these few selected frames.

2.2 Mesoscale Forecast

There are three primary approaches to surface wind prediction. The first is numerical prediction by a dynamic model. There are, however, two great barriers to such an application on a small scale. First is the problem of determining the horizontal grid spacing and vertical layering to adequately describe the terrain effects, small-scale flow patterns, and small-scale thermal stability patterns. In mountainous areas, such as at the NRTS, the characteristic lengths of flow and thermal stability patterns may be quite small. Consequently a highly sophisticated and expensive data input system is required for the model. The second barrier is the seriousness of assumptions that must be made at the boundaries. Errors at the boundaries will affect predic - tions all the way to the center of the grid in only a couple of hours at most.

The second approach bypasses the problem of numerically predicting surface winds by taking numerically predicted winds at the top of the boundary layer and relating them to the surface winds by a simple set of regression equations. This model output statistics (MOS) (Glahn, 1970) approach uses the winds predicted by the subsynoptic advection model (SAM) (Glahn et al., 1969). Unfortunately medium range prediction, which is something like 18 to 36 hours, is beyond the maximum outlook of SAM, which is 17 hours. The top of boundary layer winds from the six-level primitive equation (PE) model is

predicted through 36 hours; however, the smoothed terrain used in the current model with its 381 km, at 60°N latitude, grid spacing would not be adequate for MOS application at most western U. S. stations. Even when adequate medium range predictions of winds at the top of the boundary layer will be available in the future from PE models with much finer horizontal grids and many more layers, the use of MOS at the NRTS and many other areas will be hampered by the necessity of using, as a developmental sample for the regression equations, the upper winds from another station that is oftentimes quite distant.

The third approach, which by process of elimination is necessarily the one pursued for medium range surface wind prediction at the NRTS, is the development of empirical equations by the method of linear multiple regression. It takes two equations to predict the two components of the horizontal wind vector. The two equations may be either of two forms: U and V component equations, or direction and speed equations. The remainder of this section is concerned with which form of predictand gives the best verifications.

The multiple linear regression (MLR) technique may be used to forecast the two wind components,

$$\hat{U} = \sum_{i=0}^{p} a_i x_i$$

and

$$\hat{V} = \sum_{i=0}^{p} b_i y_i \ , \qquad (2)$$

where $x_0 = y_0 \equiv 1$. As stated by Glahn et al. (1969), in the absence of special restrictions on the a_i and b_i the component equations will give most accurate least squares fit to the total vector.

The prediction of direction in the direction-speed model is by the method of regression estimation of event probabilities (REEP) (Miller, 1964). The wind rose is divided into 'G' appropriate groups and probability equations are derived:

$$PR_g = \sum_{i=0}^{p} a_{ig} x_i , \qquad (3)$$

where

$g = 1, 2 \ldots G,$

$x_0 = 1,$ and

$$x_i = 0 \text{ or } 1 \text{ for all } i>0.$$

The wind speed is predicted by MLR equations where a separate equation is derived for each direction category.

REEP is not as objective as MLR because of the subjectivity used in dividing the predictand and predictors into groups for processing as binary variables. Each group of a given predictor is valued 0 or 1 according to whether the value of the variable falls into that group.

The two models were tested for prediction of maximum afternoon winds in winter at the NRTS. There were 582 sample cases, after removing days with missing data, from the seven winters of 1961-62 through 1967-68. The same set of predictors were screened for both models. The predictors were 700 mb U and V wind components from Boise, Lander, Great Falls, and Salt Lake City, the six possible combinations of 850 mb height gradients from among the same four cities, and the six possible combinations of sea level pressure gradients from among the stations Boise, Ida.; Pocatello, Ida.; Salt Lake City, Utah; and Dillon, Mont. The available data were from the 1200 GCT observations. Table 10 is a summary of the forecast verification.

Table 10. Error Summary for U-V Component and Speed-Direction Forecasts of CFA Maximum Afternoon Surface Winds in Winter; 582 Cases.

	Forecasts	
	U-V	Speed-Direction
rms Vector Error (mph)	11.6	11.8
Average Vector Error (mph)	10.1	9.2
Average Direction Error (deg.)	57.7	48.1
Number of Cases		
Direction Error ($\leq 30°$)	262	384
Direction Error ($>90°$)	162	146
Vector Error (≤ 3.0 mph)	88	153
Vector Error (≥ 18.0 mph)	77	94

In comparing the U-V form of forecasts to speed-direction form of forecasts, one should note a characteristic of regression estimates. The square of the simple correlation between a predictand (y) and predictor (x) is

$$r^2 = \frac{(\Sigma xy)^2}{\Sigma x^2 \Sigma y^2} \quad . \tag{4}$$

Multiplying both sides by the sums of squares of the predictand gets

$$\Sigma y^2 r^2 = \frac{(\Sigma xy)^2}{\Sigma x^2} \quad . \tag{5}$$

The right-hand member is the sum of squares of regression estimates. Therefore we have

$$\Sigma y^2 r^2 = \Sigma \hat{y}^2 \tag{6}$$

which can be shown to generalize to

$$\Sigma y^2 R^2_{y.x_1,x_2\ldots x_p} = \Sigma \hat{y}^2 \tag{7}$$

for regression of y on "p" predictors. R^2 is the multiple correlation coefficient. This expression is equivalent to

$$\sigma_y^2 \, R^2_{y.x_1,x_2\ldots x_p} = \sigma^2 \hat{y} \quad . \tag{8}$$

Since R^2 is, in general, less than "one," the variance of the predictions is less than the variance of the observed predictands. If all predictand values are positive the consequence of this characteristic in variances is a tendency to underforecast for values greater than $\bar{y}$, and to overforecast for values less than $\bar{y}$. If the distribution of "y" is about 0 in some manner the consequence will be a tendency to underforecast the $|y|$.

The former consequence applies to speed predictions in the speed-direction model, while the latter consequence applies to speed predictions from the U-V component model. In general the greatest underestimates of speed by U-V predictions occurs when the fit to direction was poorest, which is

why the rms vector error is relatively small. Since there is no general tendency to underestimate the speed in the speed-direction model, the vector errors were relatively large if the wrong direction category was predicted. We can see from table 10 that there were more good forecasts (vector error $\leq$3.0 mph) from the speed-direction forecasts, but there were also more bad forecasts (vector error $\geq$18.0 mph). The distribution of vector errors for the two models is such that the U-V forecasts yield a lower rms error. It is interesting that in spite of only three possible values in direction forecasts by REEP, the mean direction error and number of good direction forecasts were far better than the U-V forecasts of direction.

The average vector errors on 582 cases of 9 to 10 mph are better than the average vector error of 12 mph in verifying 268 forecasts from the winters 1964-65 through 1967-68 that were issued by the NRTS forecaster.

It has already been established that the method of objective forecasting at the NRTS (and the same arguments apply to a great many areas) should be that of developing linear regression equations. Forecast equations of speed and direction, because of their higher probability of a 'good' prediction, are being developed for 24 to 36 hour operational forecast use at two locations, CFA and TAN. Shorter range statistical forecasts are at best only comparable with the subjective forecaster. Another approach for shorter range forecasting would be to use the multiple time series approach of Brier et al. (1970).

The total explained variance on statistical forecasts of afternoon surface winds at the NRTS has been 30 percent to 60 percent on a number of different approaches for two data samples, winter and spring. Nevertheless, the limit on predictability of afternoon surface winds is high compared with the explained variance of only 8 percent for a set of equations derived to predict pre-dawn winds in summer. There are several reasons for the predictability limit on afternoon winds and the no-skill results on predicting pre-dawn winds in summer. These reasons, which are considered below, shall constitute the arguments for deriving only a limited set of speed and direction equations already mentioned.

A great many areas, like the NRTS, have distinct diurnal characteristics in the wind. These characteristics are often absent when relatively high energy synoptic scale patterns exist, which cases are also the most predictable. At the NRTS the diurnal pattern of wind shifts may occur from about 20 percent of the days in winter to better than 80 percent of the days in summer. The problem is that these wind shifts do not always occur the same time of day, and for reasons that

are sometimes extremely subtle. Consequently, the greater the frequency of wind shifts during the period for which prediction equations are being derived, the more "noise" is introduced into the predictand. Table 11 shows the number of wind shifts occurring in a 488 day sample from January and December for 1961 through 1968. A SW wind was defined as 180° through 260° and a NE wind as 340° through 70°. A shift was defined as when the direction was within the specified range of one of the two categories for 3 or more hours and then shifted to the opposite category for 3 or more hours. Two hours of meandering winds were allowed in the midst of the shift. The hour of the shift was the first hour of the new steady direction. Note that 50 cases or slightly better than 10 percent of the sample had wind shifts during the key 1300 through 1600 MST afternoon forecast period.

A second particular peril to forecasting surface winds in mountainous terrain is for upper winds normal to the valley axis. The critical directions of 700 mb winds over the NRTS are 290° to 310°. A winter sample of 609 1200 GCT Boise 700 mb winds from December through February for 1961-62 through 1967-68 was available for studying direction distribution. There were 156 cases from the key directions. The associated maximum afternoon surface winds at the NRTS were as follows: 340° through 40°, 69 cases; 230° through 250°, 64 cases; and other directions, mostly 260° through 330°, comprised the remaining 23 cases. A good share of these 156 cases could be discriminated statistically by using sea-level pressure gradients between SW Montana and SE Idaho; however, there were also a great many cases for which it was not at all obvious why the wind blew from the SW as opposed to the NE. These contrary cases were generally associated with near neutral sea-level pressure gradients, but a few defied significant gradients and blew from contrary quadrants.

Table 11. Frequency of Wind Shifts for January and December 1961 Through 1968 (488 Days in the Sample).

		Hour																							
From	To	1	2	3	4	5	6	7	8	9	10	11	12	13	14	15	16	17	18	19	20	21	22	23	24
NE[1]	SW	8	7	6	5	3	5	5	2	1	5	4	5	8	7	7	3	4	7	6	12	15	15	7	6
SW[2]	NE	5	3	0	3	6	5	7	3	6	17	21	10	6	5	6	8	6	6	9	8	6	0	2	3

[1] NE is 340° to 70°
[2] SW is 180° to 260°

The third and final consideration on the limit of surface wind predictability is short and simple. Many areas have frequent strong nighttime inversions with light and variable winds. These winds are extremely capricious at the NRTS and are probably so at most areas having these conditions. General wind forecast equations derived for the periods of day that frequently experience this phenomena will show no practical forecast skill. The best one might do is to develop equations to predict the occurrence of stronger winds only, and this may be done at the NRTS.

2.3 The Surface Winds at CFA

The study of surface winds at the CFA station (Yanskey et al., 1965) gives a good summary and presents wind roses for (1) the total day by season, (2) lapse conditions by season, and (3) inversion conditions by season. In a study of forecast verification at the NRTS it was found that a very high percentage of wind direction forecasts were wrong by more than 90°. The greater part of these errors were on forecasts verifying at night, which in turn was due to the general concept that in the absence of large scale storms the nighttime winds blow from the NE.

A more detailed study on wind characteristics recorded at the 20 ft level at CFA was conducted, and three more for the CFA 250 ft level, TAN 20 ft level, and TAN 150 ft levels are to follow. The data used are the hourly average winds from 1961 through 1968. Hourly average wind roses were computed for each of six 2-month periods. The wind roses do not have a smooth distribution, because before 1965 directions were recorded to only 16 points of the compass. In addition a tally of wind shifts was made. The definition of a shift from SW to NE (NE to SW) was a wind from 180° to 260° (340° to 70°) for a period of 3 hours or more, shifting to 340° to 70° (180° to 260°) for a period of 3 hours or more. Three hours of meander were allowed in the midst of the shift. The meander could include any direction, even NE or SW. The hour of the shift was recorded as the first hour for the steady direction to which the wind shifted.

Table 12 shows the wind shift statistics for four 2-month periods. Figures 17-20 show an example of the wind roses. From the wind roses and the wind shift tables two significant observations are made concerning the diurnal characteristics; this knowledge will aid in short-range forecasting for emergencies and planned tests.

Table 12. Number of Occurrences of Wind Shifts for 1961-1968.

Hour	Summer(June&July) from NE[1] to SW[2]	From SW to NE	Autumn(Oct&Nov) from NE to SW	from SW to NE	Winter(Dec&Jan) from NE to SW	from SW to NE	Spring(April&May) from NE to SW	from SW to NE
1	3	11	8	6	8	5	6	12
2	0	9	0	5	7	3	2	5
3	0	8	1	4	6	0	5	9
4	4	6	4	4	5	3	4	5
5	4	7	4	3	3	6	5	6
6	2	12	2	2	5	5	3	6
7	2	23	2	4	5	7	2	11
8	3	17	1	11	2	3	4	21
9	5	7	0	12	1	6	1	8
10	19	0	1	15	5	17	6	4
11	30	0	5	4	4	21	22	2
12	50	0	12	1	5	10	19	0
13	33	1	26	1	8	6	23	0
14	23	2	28	4	7	5	16	1
15	16	1	21	1	7	6	12	2
16	7	2	10	2	3	8	5	4
17	1	2	3	7	4	6	4	3
18	4	5	2	6	7	6	5	4
19	3	8	2	5	6	9	2	4
20	0	5	5	5	12	8	2	8
21	2	11	5	5	15	6	2	7
22	1	9	5	3	7	2	7	4
23	1	9	5	3	7	2	7	4
24	1	5	3	3	6	3	2	4

[1] NE wind is 340° to 70°

[2] SW wind is 180° to 260°

In summer (June and July) there is a marked tendency for winds to become light and variable after midnight. There was an obvious maximum of NE winds from 0800 through 1000 MST, 3 to 5 hours after sunrise. In autumn (October and November) this maximum of NE winds occurred from 1000 through 1200 MST, also 3 to 5 hours after sunrise. In winter (December and January) this maximum occurred from 1100 MST through the remainder of the daylight hours until about 1900 MST, from 3 hours after sunrise to 2 hours after sunset. In spring (April and May) the NE wind maximum is

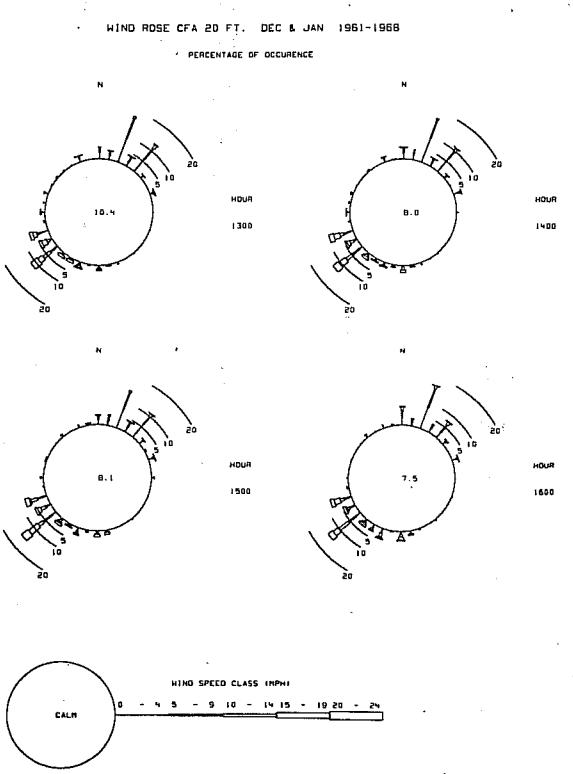

Figure 18. CFA 20-ft wind roses, December and January, 1961-1968, 1300-1600 MST.

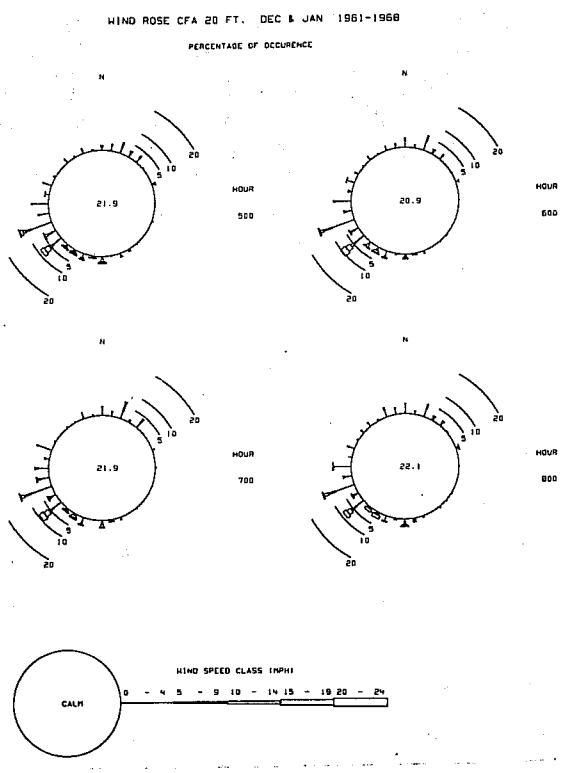

Figure 17. CFA 20-ft wind roses, December and January, 1961-1968, 0500-0800 MST.

from 0800 through 1100 MST, from 2 to 6 hours after sunrise. Note that the NE wind maximum is generally 3 to 5 hours after sunrise, except in the middle of winter when daytime heating is very poor.

The SW wind maximum in summer is from 1100 through 2000 MST with a strong persistency in SSE around to W through most of the night. There is a steady decrease in frequency of these winds through the night as more and more cases shift to NE winds or light and variable winds. This is true of all seasons but is least apparent in winter when the diurnal

effect is weakest. The autumn SW wind maximum is from 1300 through 1900 MST. The winter SW wind maximum appears to be before dawn hours but is not obvious. The winter SW winds show little diurnal characteristic, as they generally are the result of the large scale weather pattern. The maximum in spring is like summer, 1100 through 2000 MST. The maximum in February and March is 1300 through 1900 MST. In the warmest season the SW winds predominate a greater part of the day, and the period of day dominated by these winds decreases with length of day and sun's zenith angle.

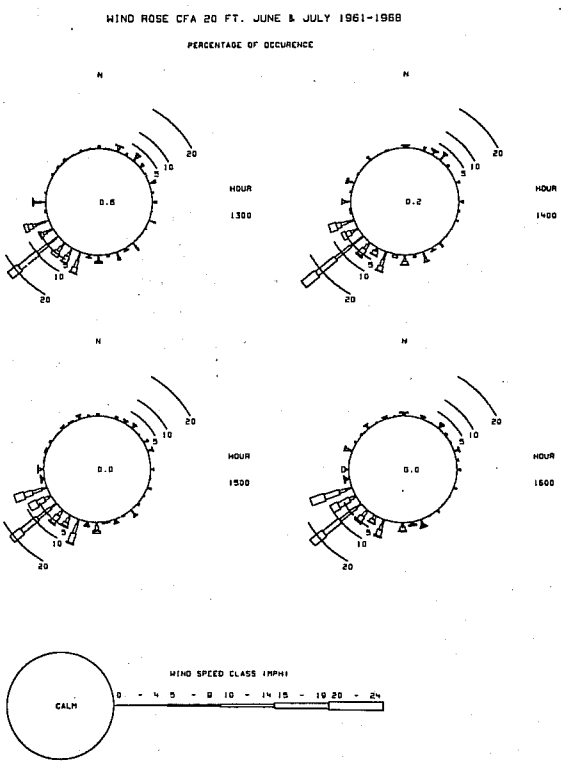

Figure 20. CFA 20-ft wind roses, June and July, 1969-1968, 1300-1600 MST.

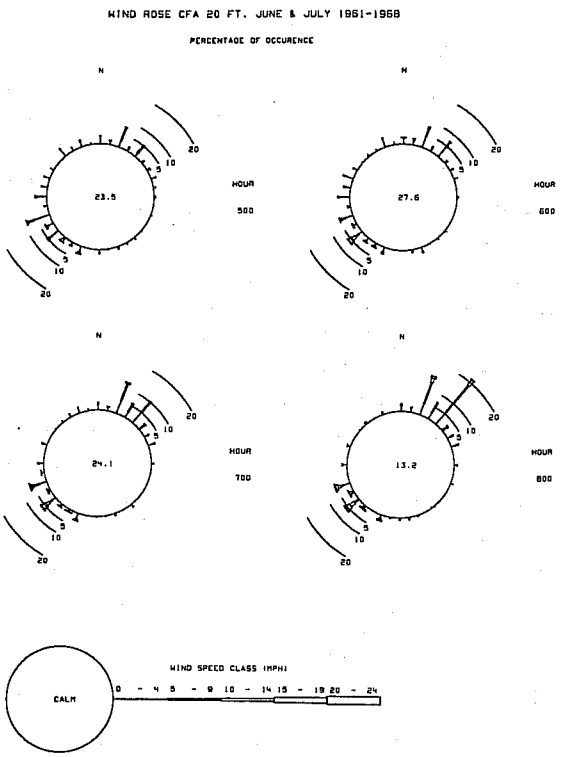

Figure 19. CFA 20-ft wind roses, June and July, 1961-1968, 0500-0800 MST.

2.4 Aircraft Wake Turbulence Interagency Study

The Federal Aviation Administration (FAA) imposed interim traffic control restrictions applicable to both the Boeing 747 and Lockheed C5A transports about 9 hours before the 747 aircraft entered commercial service. These restrictions were based on an indication that these aircraft may produce greater wake turbulence than do earlier jet transports.

In February 1970 the FAA, in cooperation with industry, the Department of Defense, the Department of Commerce, and other government agencies, undertook an accelerated evaluation of the operational impact of wake turbulence produced by large jet aircraft. With the concurring consent of the AEC sponsor, a part of the ARL-FRO staff research year was diverted to this problem. The objective of the ARL-FRO supported research was to provide quantitative data describing the wake turbulence characteristics of large, medium, and small jet transports. ARL-FRO support was required because of the unique combination of special staff skills, available computational facilities, physical facilities such as instrumented towers, and the excellent open, flat terrain for low altitude aircraft operations.

The results of the ARL-FRO support were a number of data tables and graphs of wingtip vortex size, basic shape, tangential speeds versus radial distance from the vortex center, radius of maximum speed, duration, rate of atmospheric transport, and supplemental atmospheric characteristics. Although these tables and graphs quantitized many types of vortex characteristics, their more fundamental value was to provide the basis for additional FAA interpretations and analyses. The FAA follow-on studies would attempt to relate these vortex characteristics to the characteristics of the particular test aircraft, its flight configuration, and other relevant aerodynamic parameters.

A number of valuable side benefits resulted from this priority assignment. The staff gained real competency in the use of hot wire/hot film anemometry on tall towers in the atmosphere. The calibration, handling, data recording techniques, and repair of this sophisticated and fragile instrumentation has expanded our field measurement capabilities. In addition, the ability to record, catalog, computer process, summarize, and display large quantities of data in both tables and graphs has been extended. Some new time and cost savings procedures have been adopted which will speed the preparation of tables and figures for future reports.

3. REFERENCES

Brier, Glenn W., T. H. Carpenter, and G. F. Cotton (1970), Time series analysis and cycles in geophysical phenomena, paper presented at the I.C.R.I. Conference, Noordwijk, The Netherlands, June 1970.

ESSA Tech. Memo. (1970), Atmospheric transport and diffusion in the planetary boundary layer, Air Resources Laboratories semiannual research program review for the Division of Reactor Development and Technology, USAEC, ERLTM-ARL-9 (1968), 60 pp; ERLTM-ARL-20 (1970), 65 pp; ERLTM-ARL-17 (1970), 44 pp. (unpublished reports), NOAA Air Resources Labs. Silver Spring, Md.

Glahn, Harry R. (1970), A method for predicting surface winds, ESSA Technical Memorandum WBTS-TDL-29, 18 pp. (unpublished report), NOAA Air Resources Labs. Silver Spring, Md.

Glahn, H. R., D. A. Lowry, and G. W. Hollenbaugh (1969), An operational subsynoptic advection model, ESSA Technical Memorandum WBTM-TDL-23, 26 pp. (unpublished report), NOAA Air Resources Labs. Silver Spring, Md.

Miller, R. G. (1964), Regression estimation of event probabilities, Tech. Report No. 1, Contract Cwb-10704, The Travelers Research Center, Hartford, Conn. 153 pp.

Yanskey, George R., Earl H. Markee, Jr., and Alden P. Richter (1965), Climatography of the National Reactor Testing Station, IDO-12048, February 49 through February 65. AEC Operations Office, Idaho Falls, Idaho.

APPENDIX A

Review of Reactor Safety Analysis Reports

The Air Resources Laboratories in Silver Spring, Maryland, and the Field Office in Idaho have continued to take an active part in the review of reactor safety analysis reports as well as consultations during the preparation of the reports. In addition, written comments have been prepared for the Division of Reactor Licensing through the Division of Reactor Development and Technology of the AEC:

1. Midland Plant Units 1 and 2, Consumers Power Company Preliminary Safety Analysis Report, Amendment No. 5, dated November 7, 1969.
2. Fort Calhoun Station Unit No. 1, Omaha Public Power District Final Safety Analysis Report, Volumes 1 through 5, dated November 28, 1969.
3. Beaver Valley Power Station, Duquesne Light Company Preliminary Safety Analysis Report, Amendment 2, dated December 17, 1969.
4. Indian Point Nuclear Generating Unit No. 2, Consolidated Edison Company of New York, Inc. Final Facility Description and Safety Analysis Report, Amendment No. 12, dated November 21, 1969.
5. Midland Plant Units 1 and 2, Consumers Power Company Preliminary Safety Analysis Report, Amendment No. 6, dated December 29, 1969.
6. Indian Point Nuclear Generating Unit No. 2, Consolidated Edison Company of New York, Inc. Final Facility Description and Safety Analysis, Amendment No. 12, dated November 21, 1969, and Amendment No. 14, dated January 27, 1970.
7. H. B. Robinson Unit 2, Carolina Power and Light Company Final Facility Description and Safety Analysis Report, Amendment No. 11, dated December 2, 1969.
8. Millstone Nuclear Power Station, The Conneticut Light and Power Company Preliminary Safety Analysis Report, Amendment No. 6, dated April 10, 1970.
9. Davis-Besse Nuclear Power Station, Toledo Edison Company Preliminary Safety Analysis Report, Amendment No. 3, dated April 16, 1970.

10. Limerick Generating Station, Units 1 and 2, Philadelphia Electric Company Preliminary Safety Analysis Report, Volumes 1 through 5, dated February 26, 1970.

11. Pilgrim Nuclear Power Station Final Safety Analysis Report, Volumes 1 through 5, dated December 31, 1969.

12. Vermont Yankee Nuclear Power Station Final Safety Analysis Report, Volumes 1 through 4, dated December 31, 1969.

13. Trojan Nuclear Plant, Portland General Electric Company Preliminary Safety Analysis Report, Amendment No. 5, dated April 16, 1970.

14. Oconee Nuclear Station, Units 1, 2, and 3, Duke Power Company Final Safety Analysis Report, Amendment No. 15, dated July 9, 1970 and Amendment No. 16, dated July 23, 1970.

A1. PUBLICATIONS AND REPORTS

Pack, D. H., J. K. Angell, M. Hodges, W. Hoecker (1969), Tetroon Flights in Los Angeles, California - 1969, ESSA Tech. Memo. ERLTM-ARL-19, 27 pp. (unpublished report), Silver Spring, Md.

Wendell, L. L. (1969), A study of large-scale atmospheric turbulent kinetic energy in wave-number frequency space, Tellus 21, 760-788.

Wendell, L. L. (1970), (co-author), On the spectral distribution of large-scale atmospheric kinetic energy Journal of Atmospheric Sciences, 27, 359-375.

A2. LABORATORY PERSONNEL

Silver Spring, Maryland

David H. Slade, meteorologist, transferred from ESSA to the Fallout Studies Branch, Division of Biology and Medicine, U. S. Atomic Energy Commission, Germantown, Md. on February 7, 1970.

Idaho Falls, Idaho

Mr. Wallace Passey, scientific assistant, was hired temporarily for the period March 31, 1970 to May 5, 1970.

Mr. William Howell, electronic technician, was hired temporarily beginning April 15, 1970.

Mr. Frank Mahoney, mathematician, was hired on a WAE (when actually employed) basis beginning June 1, 1970.

Mr. Norman Ricks, student assistant, was hired on a WAE basis beginning June 16, 1970.